PLABIC LINKS, QUIVERS, AND SKEIN RELATIONS

PAVEL GALASHIN AND THOMAS LAM

ABSTRACT. We study relations between cluster algebra invariants and link invariants.

First, we show that several constructions of *positroid links* (permutation links, Richardson links, grid diagram links, plabic graph links) give rise to isotopic links. For a subclass of permutations arising from concave curves, we also provide isotopies with the corresponding Coxeter links.

Second, we associate a *point count polynomial* to an arbitrary locally acyclic quiver. We conjecture an equality between the top a-degree coefficient of the HOMFLY polynomial of a plabic graph link and the point count polynomial of its planar dual quiver. We prove this conjecture for leaf recurrent plabic graphs, which includes reduced plabic graphs and plabic fences as special cases.

1. INTRODUCTION

In recent years, intriguing connections between knot theory and the theory of cluster algebras have been developed. Shende–Treumann–Williams–Zaslow [STWZ19] found cluster structures on certain moduli spaces of sheaves microsupported on a Legendrian link. Fomin–Pylyavskyy–Shushtin–Thurston [FPST22] studied the relation between quiver mutation and morsifications of algebraic links. Casals–Gorsky–Gorsky–Simental [CGGS21] and Mellit [Mel19] studied braid varieties associated to positive braid words; cluster structures on these spaces are the subject of ongoing works [CGG+22, GLSBSa, GLSBSb]. Other connections can be found e.g. in [HI15, Mul16, LS19, BMS21, CW22].

The goal of this work is to compare knot invariants and cluster algebra invariants. The starting point is our earlier work [GL20] on *open positroid varieties* $\mathring{\Pi}_\pi$ [KLS13], which are certain distinguished subvarieties of the Grassmannian equipped with a cluster structure [GL19] (see also [Sco06, MS16, Lec16, SSBW19]). In [GL20], we associated a *positroid link* L_π to each open positroid variety $\mathring{\Pi}_\pi$, and constructed an isomorphism between the cohomology of $\mathring{\Pi}_\pi$ and the top a-degree part of the Khovanov–Rozansky triply-graded link homology [KR08a, KR08b, Kho07] of L_π. In subsequent work [GL21], we further developed this connection by defining *positroid Catalan numbers* as certain Euler characteristics of open positroid varieties. This invariant was studied for a subclass of permutations arising from concave curves, using a Dyck path recursion that did not require explicit mention of the cluster structure on $\mathring{\Pi}_\pi$, or of the positroid link L_π.

(a) L4a1   (b) L_π^{perm} (c) L_π^{tor} (d) $\mathbb{T} \hookrightarrow \mathbb{R}^3$
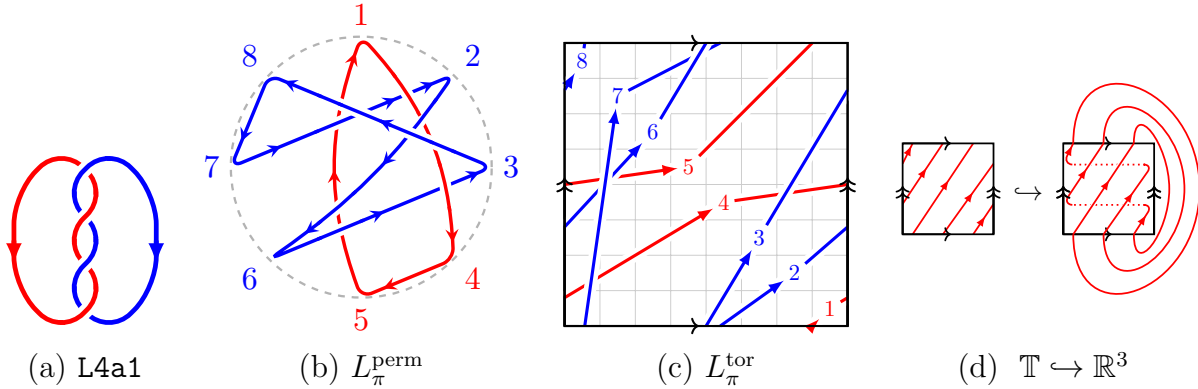
FIGURE 1. The links L4a1$\cong L_\pi^{\mathrm{perm}} \cong L_\pi^{\mathrm{tor}}$ for π given by (2.1).

The initial motivation of this work is to explain our positroid recursion in the broader setting of *plabic (i.e., planar bicolored) graphs*, making an explicit connection to recursions for quivers and for links. Plabic graphs were introduced by Postnikov [Pos06] who also speculated on the relation with cluster algebras. To an arbitrary plabic graph G one can associate a *plabic graph link* L_G^{plab} introduced in [FPST22, STWZ19]. On the other hand, the set of equivalence classes of *reduced* plabic graphs is in bijection with open positroid varieties, to which we associated positroid links in [GL20].

In the first part of this work, we establish (Theorem 2.5) that the various links associated to $\mathring{\Pi}_\pi$ are isotopic, including the positroid link L_π and the corresponding plabic graph link L_G^{plab}. In the second part of this work, we study the relation between the point count function of a quiver Q and the HOMFLY polynomial $P(L; a, z)$ of a link. We introduce a class of *simple* plabic graphs. Our main conjecture (Conjecture 2.8) states that for a simple plabic graph G, the point count of the planar dual quiver Q_G is equal to the top a-degree part of the HOMFLY polynomial of L_G^{plab}. We show (Theorem 2.9) that this conjecture holds for the class of *leaf recurrent* plabic graphs, that includes reduced plabic graphs and plabic fences. We interpret and generalize the locally acyclic recursion for positroids [MS16] in terms of the HOMFLY skein relation.

Acknowledgments. The second author thanks David Speyer for the previous collaborations [LS22, LS21], which have influenced this work. The authors thank Eugene Gorsky for explanations related to [CGGS21].

2. MAIN RESULTS

Let $\pi \in S_N$ be a permutation. For simplicity, we assume that π has no fixed points, i.e., $\pi(i) \neq i$ for all $i \in [N] := \{1, 2, \ldots, N\}$.

In [GL20], we described a way to associate a *positroid link* L_π to such π. The number of components of L_π is given by the number $\mathrm{c}(\pi)$ of cycles of π. Our running example will be

$$(2.1) \qquad \pi = \begin{pmatrix} 1 & 2 & 3 & 4 & 5 & 6 & 7 & 8 \\ 4 & 6 & 8 & 5 & 1 & 3 & 2 & 7 \end{pmatrix},$$

written in two-line notation, with different colors representing different cycles of π. We have $N = 8$ and $\mathrm{c}(\pi) = 2$. The associated positroid link L_π is shown in Figure 1(a); it appears under the name L4a1 in the Thistlethwaite Link Table [KAT1].

(a) L_π^{tor} (b) $\tilde{L}_\pi^{\mathrm{grid}}$ (c) L_π^{grid} (d) L_π'
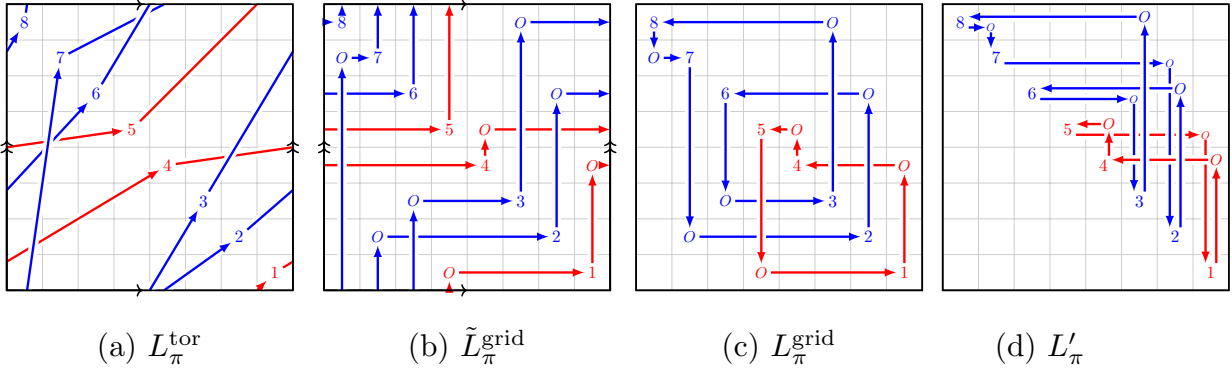
FIGURE 2. Toric grid links; see Remark 2.2 and Section 4.3.

2.1. **Positroid links.** Our first result relates several different representations of the link L_π, confirming the conjectures of [GL20, GL21]. We start by giving a brief overview of these descriptions; see Sections 3 and 4 for full details.

2.1.1. *Permutation link.* Draw N points labeled $1, 2, \ldots, N$ on the circle in clockwise order. Draw a line segment connecting i to $\pi(i)$, for each $i \in [N] := \{1, 2, \ldots, N\}$. If two line segments $[i, \pi(i)], [j, \pi(j)]$ cross for some $i, j \in [N]$ such that $\pi(i) < \pi(j)$, then the segment $[j, \pi(j)]$ is drawn above $[i, \pi(i)]$; see Figure 1(b). The union of these segments gives rise to a link diagram. We refer to the resulting link as the *permutation link* of π, denoted L_π^{perm}. Orienting each line segment from i to $\pi(i)$ induces an orientation on L_π^{perm}.

2.1.2. *Toric permutation link.* Let $\mathbb{T} := \mathbb{R}^2/\mathbb{Z}^2$ be the torus. Consider its fundamental domain $[0, 1]^2$ which we view as a square subdivided into N^2 boxes of size $\frac{1}{N} \times \frac{1}{N}$. We denote by $b_{i,j}$, $1 \le i, j \le N$, the box whose upper right corner has coordinates $\frac{1}{N}(i, j)$. For each $i \in [N]$, place a dot d_i in box $b_{i,N+1-i}$. Draw an arrow (in $\mathbb{T}$) in the northeast direction from d_i to $d_{\pi(i)}$ for each $i \in [N]$. When two such arrows cross, the arrow with the higher slope is drawn above the arrow with the lower slope. We obtain a planar diagram of an oriented link L_π^{tor} drawn on the surface of $\mathbb{T}$; see Figure 1(c). Embedding $\mathbb{T}$ inside $\mathbb{R}^3$ in a standard way (Figure 1(d)), we may view L_π^{tor} as a link in $\mathbb{R}^3$.

Remark 2.1. Viewing L_π^{tor} as drawn on the surface of $\mathbb{T}$ (resp., in a solid torus $S^1 \times [0, 1]$) contains more information—it gives rise to a certain elliptic Hall algebra element [SV13, BS12] (resp., to a symmetric function [Tur88]) with deep connections to Khovanov–Rozansky homology. We aim to pursue this direction in an upcoming paper.

Remark 2.2. We may also view L_π^{tor} as coming from a *grid diagram* (see, e.g., [OSS15]). The grid diagram of π is obtained by placing an X in box $b_{i,N+1-i}$ and an O in box $b_{i,N+1-\pi(i)}$ for each $i \in [N]$. We then connect the X's and the O's by horizontal and vertical segments, always drawing the vertical segments above the horizontal ones. More precisely, to a given grid diagram, we can associate two links. First, a *toric grid link* $\tilde{L}_\pi^{\mathrm{grid}}$, drawn on the surface of $\mathbb{T}$, is obtained by drawing a horizontal arrow from O to X pointing right in each row, and a vertical arrow from X to O pointing up in each column; see Figure 2(b). (In Figure 2, for each $i \in [N]$, we place an i instead of an X in box $b_{i,N+1-i}$.) Second, a *planar grid link* L_π^{grid}, whose planar diagram is drawn inside $[0, 1]^2$, is obtained by drawing a horizontal arrow from O to X in each row, and a vertical arrow from X to O in each column, but in this case

$$\beta(w) = \sigma_3\sigma_2\sigma_1\sigma_4\sigma_3\sigma_2\sigma_5\sigma_4\sigma_3\sigma_7\sigma_6\sigma_5\sigma_4 \qquad \beta(v)^{-1} = \sigma_2^{-1}\sigma_6^{-1}\sigma_3^{-1}$$

Richardson braid $\beta_{v,w} = \beta(w) \cdot \beta(v)^{-1}$ Richardson link $L_{v,w}^{\mathrm{Rich}}$
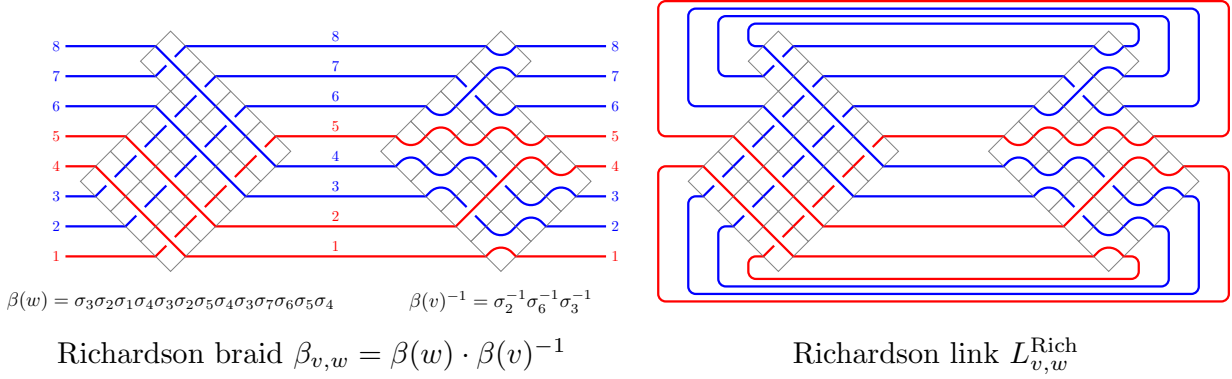
FIGURE 3. A Richardson braid (left) and a Richardson link (right) defined in Section 2.1.3.

the arrows are not allowed to cross the boundaries of $[0,1]^2$; see Figure 2(c). As explained in [OSS15, Section 3.2], these two links are isotopic to each other. It is easy to see that the toric grid link $\tilde{L}_\pi^{\mathrm{grid}}$ is also isotopic to L_π^{tor}.

2.1.3. *Richardson link.* A permutation $w \in S_N$ is called *k-Grassmannian* if $w(1) < \cdots < w(N-k)$ and $w(N-k+1) < \cdots < w(N)$. We denote by $S_N^{(k)}$ the set of k-Grassmannian permutations. The permutation π can be uniquely decomposed as the product $\pi = wv^{-1}$ for some $1 \le k \le N-1$ and some pair $(v,w) \in S_N \times S_N^{(k)}$ such that $v \le w$ in the Bruhat order on S_N. For the permutation π given by (2.1), we get that $k = 4$ and[1]

$$v = \begin{pmatrix} 1 & 2 & 3 & 4 & 5 & 6 & 7 & 8 \\ 1 & 4 & 2 & 3 & 5 & 7 & 6 & 8 \end{pmatrix}, \quad w = \begin{pmatrix} 1 & 2 & 3 & 4 & 5 & 6 & 7 & 8 \\ 4 & 5 & 6 & 8 & 1 & 2 & 3 & 7 \end{pmatrix}.$$

Here, the colors represent the cycles of $\pi = wv^{-1}$. Let $\beta(v), \beta(w)$ be the positive braid lifts of v, w to the braid group of S_N. Consider the *Richardson braid* $\beta_{v,w} := \beta(w) \cdot \beta(v)^{-1}$ shown in Figure 3(left). Taking the *braid closure* of $\beta_{v,w}$, we obtain the *Richardson link* $L_{v,w}^{\mathrm{Rich}} = L_\pi^{\mathrm{Rich}}$ shown in Figure 3(right). We orient the strands of $\beta_{v,w}$ from right to left; cf. Figure 14(left).

Remark 2.3. It is well known that k-Grassmannian permutations are in bijection with Young diagrams that fit inside a $k \times (N-k)$ rectangle. Thus, in Figure 3(left), we arrange the crossings in $\beta(w)$ into a (rotated) Young diagram. The condition that $v \le w$ in the Bruhat order implies that a reduced word for v is a subword of a reduced word for w, and thus we represent $\beta(v)$ in Figure 3(left) by replacing some of the crossings in $\beta(w)$ with "elbows."

The above recipe was used in [GL20] more generally for pairs $v \le w$ where w is not necessarily k-Grassmannian.

2.1.4. *Plabic link.* A *plabic graph* is a non-empty planar graph G embedded in a disk with vertices colored black and white; see [Pos06]. A *strand* in G is a path that makes a sharp right turn at each black vertex and a sharp left turn at each white vertex. We assume that the graph G has N boundary vertices, all of which have degree 1 and are labeled $1, 2, \ldots, N$

---

[1]Our convention for multiplying permutations is right-to-left, i.e., $\pi(j) = w(v^{-1}(j))$ for all $j \in [N]$.
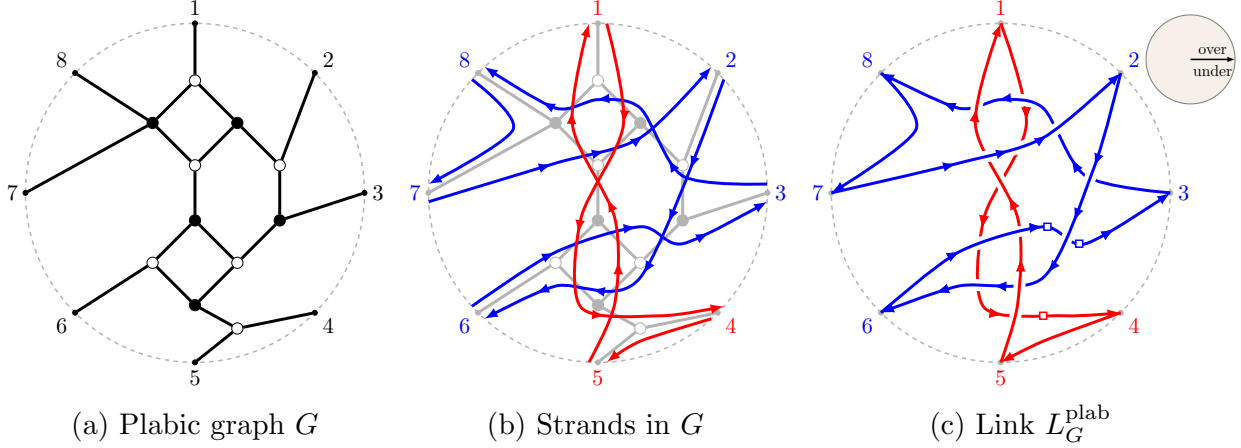
(a) Plabic graph G (b) Strands in G (c) Link L_G^{plab}

FIGURE 4.   Converting a plabic graph G into the plabic graph link L_G^{plab}.
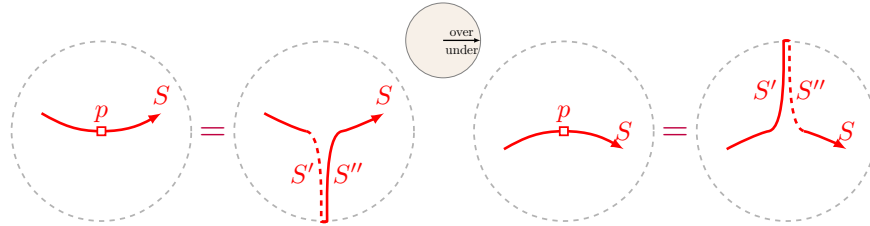

FIGURE 5.   For every point p on a strand S satisfying $\arg(S, p) = 0$, we insert a strand segment going to the boundary and back; see Section 2.1.4.

in clockwise order. An example of a plabic graph G is shown in Figure 4(a), and the strands in G are shown in Figure 4(b).

The following description of the *plabic graph link* L_G^{plab}, or *plabic link* for short, can be deduced from [A'C99, STWZ19, FPST22] by breaking the symmetry following [Hir02]. (See Section 3.4 for a more invariant description.) The planar diagram of L_G^{plab} will consist of the union of the strands of G. To specify the overcrossings, let p be an intersection point of two strands S_1, S_2 in G. The tangent vector to S_1 (resp. S_2) at p can be considered a vector in the complex plane, and we let $\arg(S_1, p) \in [0, 2\pi)$ (resp. $\arg(S_2, p) \in [0, 2\pi)$) denote the argument of this vector. We assume that $0 < \arg(S_1, p) \neq \arg(S_2, p) < 2\pi$. Then S_1 is drawn above S_2 if $\arg(S_2, p) > \arg(S_1, p)$, otherwise S_1 is drawn below S_2.

A technical extra step is required to finalize the construction of L_G^{plab}; see Figure 5. Consider a point p on a strand S such that $\arg(S, p) = 0$, i.e., such that S is directed to the right at p. We add an extra segment S' to S traveling from p to the boundary of the disk followed by a segment S'' traveling from the boundary back to p. In the neighborhood of p, S looks like a plot of a function. If this function is "concave up" at p (i.e., has positive second derivative), then S' (resp., S'') is drawn below (resp., above) all other strands. If S is "concave down" at p then S' (resp., S'') is drawn above (resp., below) all other strands.

Finally, each boundary vertex of G is an endpoint of exactly two strands (one outgoing and one incoming). We join these endpoints together and obtain a planar diagram of a link denoted L_G^{plab}. See Figure 4(c), where the points p such that $\arg(S, p) = 0$ are marked by the symbol ▫.
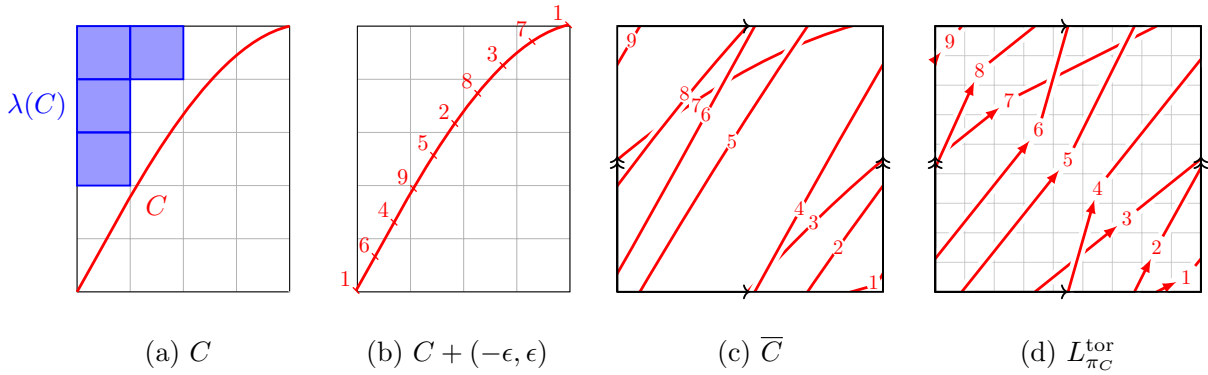
FIGURE 6.   Converting a concave curve C into the link $L^{\text{tor}}_{\pi_C}$ for some $\pi_C \in S_N$; see Example 2.4.

The strands in G that start and end at the boundary vertices give rise to the *strand permutation* π_G of G. In this subsection, we will assume that G is *reduced*, i.e., that G has the minimal possible number of faces among all graphs with a given strand permutation. Importantly, in Section 2.2, we will drop this assumption. Postnikov [Pos06] showed that for any $\pi \in S_N$, there exists a reduced plabic graph G with strand permutation $\pi_G = \pi$. For example, for π given by (2.1), one can take G to be the graph in Figure 4(a). Up to isotopy, the resulting link L^{plab}_G depends only on π and is denoted L^{plab}_π.

2.1.5. *Coxeter link.* In [GL21, Section 6], we studied *concave permutations*, defined as follows. Choose a generic concave curve C inside a $k \times (N - k)$ rectangle connecting $(0, 0)$ to $(k, N - k)$ as in Figure 6(a). We will shift it by the vector $(-\varepsilon, \varepsilon)$ for some small $\varepsilon > 0$ as in Figure 6(b). Under the natural projection $\mathbb{R}^2 \to \mathbb{T} = \mathbb{R}^2/\mathbb{Z}^2$, the curve $C + (-\varepsilon, \varepsilon)$ projects to a curve $\overline{C}$ in the unit square $[0, 1]^2$. For each self-intersection of $\overline{C}$, we draw the segment of the higher slope above the segment of the lower slope; see Figure 6(c). The resulting link diagram is isotopic to L^{tor}_π for a permutation $\pi = \pi_C \in S_N$ which can be explicitly read off from $\overline{C}$ as follows. Label the intersection points of $\overline{C}$ with the $y = 1 - x$ diagonal of $[0, 1]^2$ by $d_1, d_2, \ldots, d_N$, proceeding in the northwest direction. Thus, $d_1 = (1 - \varepsilon, \varepsilon)$ is the projection of the starting and ending points of $C + (-\varepsilon, \varepsilon)$. In Figure 6(c), we represent each point d_i by i. Since C was generic, we assume that the points $d_1, d_2, \ldots, d_N$ are pairwise distinct. The permutation π_C is defined so that each segment of C connects (in the northeast direction) d_i to $d_{\pi(i)}$ for some $i \in [N]$. See Figure 6(d). We refer to permutations that can be obtained in this way as *concave permutations*. They form a subclass of the class of *repetition-free permutations* introduced in [GL21].

Let $\lambda_C = (\lambda_1, \lambda_2, \ldots, \lambda_k)$ be the Young diagram inside the $k \times (N - k)$ rectangle consisting of all unit boxes strictly above C, shown in Figure 6(a). Consider a sequence $\mathbf{a}(C) = (a_2, \ldots, a_k)$ given by $a_i := \lambda_{i-1} - \lambda_i$ for $2 \le i \le k$. The *Coxeter link* L^{Cox}_C is the closure of the braid

$$(2.2) \qquad \beta(\mathbf{a}(C)) := \ell_2^{a_2} \cdots \ell_k^{a_k} \cdot \sigma_1 \cdots \sigma_{k-1},$$

where $\sigma_1, \ldots, \sigma_{k-1}$ are the standard braid group generators of the braid group of S_k, and $\ell_i = \sigma_{i-1} \cdots \sigma_1 \cdot \sigma_1 \cdots \sigma_{i-1}$ are the Jucys–Murphy elements.
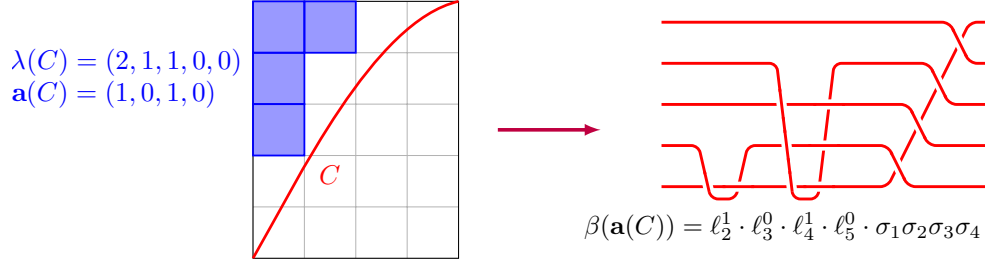
$$\lambda(C) = (2, 1, 1, 0, 0)$$
$$\mathbf{a}(C) = (1, 0, 1, 0)$$

$$\beta(\mathbf{a}(C)) = \ell_2^1 \cdot \ell_3^0 \cdot \ell_4^1 \cdot \ell_5^0 \cdot \sigma_1 \sigma_2 \sigma_3 \sigma_4$$

FIGURE 7. Converting a concave curve C into the Coxeter braid $\beta(\mathbf{a}(C))$.

Example 2.4. Let C be the curve shown in Figures 6 and 7. We have $k = 5$ and $N = 9$. The permutation $\pi_C = \begin{pmatrix} 1 & 2 & 3 & 4 & 5 & 6 & 7 & 8 & 9 \\ 6 & 8 & 7 & 9 & 2 & 4 & 1 & 3 & 5 \end{pmatrix}$ can be read off from the labels[2] in Figure 6(b): in cycle notation, π_C is given by $\pi_C = (1\,6\,4\,9\,5\,2\,8\,3\,7\,1)$. We have $\lambda_C = (2, 1, 1, 0, 0)$, $\mathbf{a}(C) = (1, 0, 1, 0)$, and $\beta(\mathbf{a}(C)) = \ell_2 \ell_4 \sigma_1 \sigma_2 \sigma_3 \sigma_4$; see also [GL21, Figure 13].

Coxeter links and their Khovanov–Rozansky homology have previously been studied in relation to flag Hilbert schemes and generalized shuffle conjectures [OR17, GN15, GNR21, BHM$^+$21]; see also [GL21, Section 7.2].

The following is our first main result.

Theorem 2.5. *Let $\pi \in S_N$ be a permutation without fixed points. Then the links L_π^{perm}, L_π^{tor}, L_π^{Rich}, and L_π^{plab} are all isotopic. If $\pi = \pi_C$ for some concave curve C then each of these links is also isotopic to L_C^{Cox}.*

We refer to any one of the above links as the *positroid link* of π.

Remark 2.6. Recently, isotopies between the Richardson link L_π^{Rich} and some other closely related links (namely, closures of juggling braids, cyclic rank matrix braids, and Le-diagram braids) were independently constructed in [CGGS21]. Isotopies between cyclic rank matrix links and plabic graph links have also been observed in [STWZ19].

2.2. **Quiver point count and the HOMFLY polynomial.** In this subsection, we consider not necessarily reduced plabic graphs G. Throughout the paper, we assume that the interior faces of G are simply connected, i.e., that no interior face of G contains another connected component of G inside of it. For simplicity, we also assume that each plabic graph G is *trivalent*, i.e., that each interior vertex of G has degree 3. (Recall that the boundary vertices of G are always required to have degree 1.)

Let G be a (trivalent) plabic graph. The planar dual of G is naturally a directed graph denoted Q_G. Explicitly, place a vertex of Q_G inside each *interior face* of G (i.e., a face not adjacent to the boundary of the disk). For every edge e of G whose endpoints are of different color and such that the two faces F, F' adjacent to e are both interior, Q_G contains an arrow between F and F'. (These two faces F, F' may or may not be equal.) The direction of the arrow is chosen so that the white endpoint of e is on the left as one moves along this arrow. See Figure 8.

The following definition is crucial for our analysis.

---

[2]The labels in Figure 6(b) are chosen in such a way that when we project C to the unit square, they become ordered along the diagonal $y = 1 - x$; see Figure 6(c).
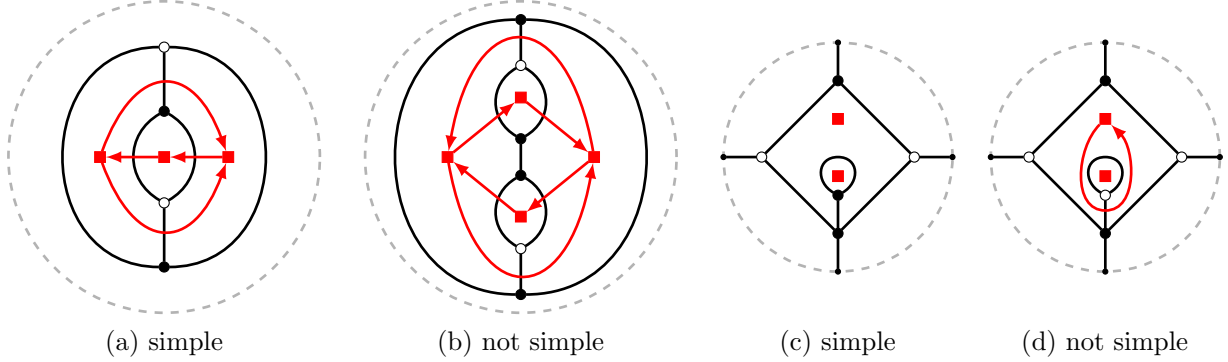
FIGURE 8. Examples of simple and non-simple plabic graphs G (black) and their planar duals Q_G (red).

Definition 2.7. A plabic graph G is called *simple* if the directed graph Q_G is a *quiver*, i.e., contains no directed cycles of length 1 and 2.

For example, the plabic graph G in Figure 8(b) is not simple since Q_G contains a pair of opposite arrows. The graph G in Figure 8(d) is not simple since Q_G contains a loop arrow. The graphs in Figure 8(a,c) are simple.

To every *locally acyclic*[3] quiver Q (see Section 5.1), we associate a rational function $R(Q; q)$ called the *point count rational function*. It can be computed via an explicit recurrence relation: see (5.2) and (5.11). The function $R(Q; q)$ has the following interpretation in terms of *cluster algebras* [FZ02]; see Section 5.1 for the relevant definitions. Let Q be a quiver with n vertices. Consider an ice quiver $\widetilde{Q}$ with m frozen vertices and mutable part Q, and assume that the rows of the $(n + m) \times n$ exchange matrix $\widetilde{B}(\widetilde{Q})$ of $\widetilde{Q}$ span $\mathbb{Z}^n$ over $\mathbb{Z}$. Then the cluster algebra $\mathcal{A}(\widetilde{Q})$ gives rise to a *cluster variety* $\mathcal{X}(\widetilde{Q})$, and its point count over a finite field $\mathbb{F}_q$ with q elements (for q a prime power) is given by

$$\#\mathcal{X}(\widetilde{Q})(\mathbb{F}_q) = (q-1)^m \cdot R(Q; q);$$

see Proposition 5.7.

A typical example of this phenomenon occurs when G is a reduced plabic graph: then, by [GL19], $\mathcal{A}(\widetilde{Q}_G)$ is the coordinate ring of the associated *open positroid variety* Π_G° inside the Grassmannian [Pos06, KLS13]. In particular, $(q-1)^{N-c(G)} R(Q_G; q)$ counts the number of points in $\Pi_G^\circ(\mathbb{F}_q)$, where N is the number of boundary vertices of G and $c(G)$ is the number of connected components of G.

Given an (oriented) link L, one can define a Laurent polynomial $P(L) = P(L; a, z)$ called the *HOMFLY polynomial* [FYH+85, PT87] of L. It is defined by the skein relation

$$(2.3) \qquad aP(L_+) - a^{-1}P(L_-) = zP(L_0) \quad \text{and} \quad P(\bigcirc) = 1.$$

Here, $\bigcirc$ denotes the unknot and L_+, L_-, L_0 are any three links whose planar diagrams locally differ as follows.

$$L_+ \qquad L_- \qquad L_0$$

---
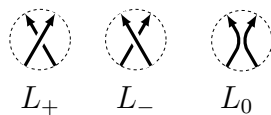
[3]We call a quiver locally acyclic if it satisfies the "Louise condition" of [MS16, LS22]. This is stronger than the notion of local acyclicity used in [Mul13].
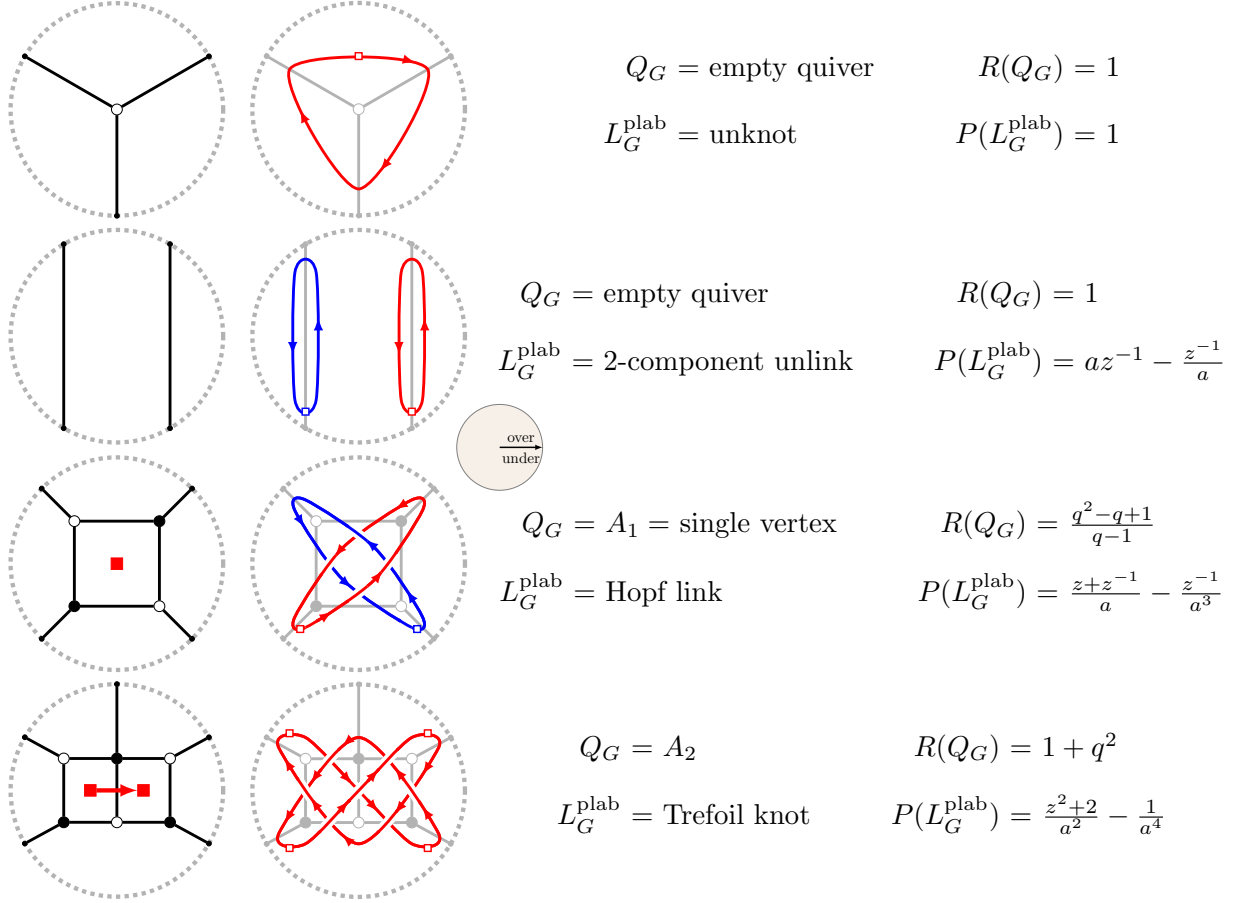
Q_G = empty quiver $R(Q_G) = 1$

L_G^{plab} = unknot $P(L_G^{\text{plab}}) = 1$

Q_G = empty quiver $R(Q_G) = 1$

L_G^{plab} = 2-component unlink $P(L_G^{\text{plab}}) = az^{-1} - \frac{z^{-1}}{a}$

$Q_G = A_1$ = single vertex $R(Q_G) = \frac{q^2 - q + 1}{q - 1}$

L_G^{plab} = Hopf link $P(L_G^{\text{plab}}) = \frac{z + z^{-1}}{a} - \frac{z^{-1}}{a^3}$

$Q_G = A_2$ $R(Q_G) = 1 + q^2$

L_G^{plab} = Trefoil knot $P(L_G^{\text{plab}}) = \frac{z^2 + 2}{a^2} - \frac{1}{a^4}$

FIGURE 9. Small plabic graph quivers Q_G, links L_G^{plab}, point counts $R(Q_G; q)$, and HOMFLY polynomials $P(L^{\text{plab}}; a, z)$ illustrating Conjecture 2.8.

For a (not necessarily reduced) plabic graph G we let L_G^{plab} be the corresponding plabic graph link, defined as in Section 2.1. Following [GL20], we let $P^{\text{top}}(L; q)$ be obtained from the top a-degree term of $P(L; a, z)$ by substituting $a := q^{-\frac{1}{2}}$ and $z := q^{\frac{1}{2}} - q^{-\frac{1}{2}}$. The following conjecture generalizes [GL20, Theorem 1.11] (see also [STZ17, STWZ19]).

Conjecture 2.8. *Let G be a simple plabic graph with* $c(G)$ *connected components. Then we have*

(2.4) $$R(Q_G; q) = (q - 1)^{c(G) - 1} P^{\text{top}}(L_G^{\text{plab}}; q).$$

For examples, see Figure 9, Example 5.11, and Section 9.

When the plabic graph G is reduced, Conjecture 2.8 becomes [GL20, Theorem 1.11]. We present a different proof in Section 7.2 by giving a plabic graph interpretation of the HOMFLY skein relation (2.3). More generally, in Section 7.1, we introduce a class of *leaf recurrent plabic graphs* and prove Conjecture 2.8 for them.

Theorem 2.9. *Conjecture 2.8 holds for leaf recurrent plabic graphs.*

The fact that reduced plabic graphs are leaf recurrent was shown in [MS16, Remark 4.7]. Another natural subclass of leaf recurrent plabic graphs are the *plabic fences* of [FPST22, Section 12]. A *plabic fence* is a plabic graph obtained by drawing k horizontal strands and
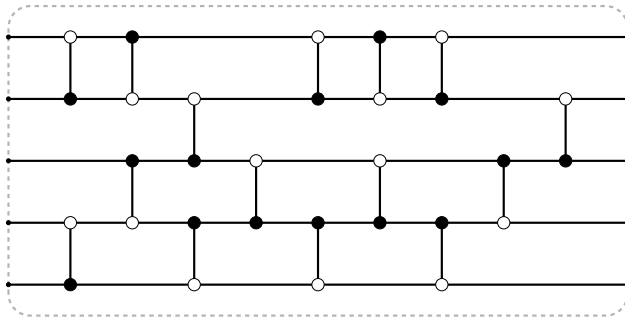
FIGURE 10.   A plabic fence.

inserting an arbitrary number of black-white and white-black bridges between them; see Figure 10 for an example and Section 7.3 for a precise definition.

Proposition 2.10. *Reduced plabic graphs and plabic fences are leaf recurrent. In particular, Conjecture 2.8 holds for these classes of plabic graphs.*

This result gives a new proof of [GL20, Theorem 1.11].

A primary difficulty in showing Conjecture 2.8 in full generality comes from the examples described in Sections 9.1 and 9.2. Section 9.1 explains that the simple plabic graph G in Figure 8(a) is not leaf recurrent. The quiver Q_G is locally acyclic (in fact, it is mutation equivalent to an acyclic quiver), and thus the point count polynomial $R(Q_G; q)$ can be easily checked to coincide with $P^{\text{top}}(L_G^{\text{plab}}; q)$. Section 9.2 describes a simple plabic graph G such that Q_G is not locally acyclic, in which case the task of computing $R(Q_G; q)$ becomes much harder.

Both sides of (2.4) are rational functions in q which are specializations of rational functions in (q, t) arising from the cohomology of cluster varieties on the one hand and Khovanov–Rozansky link homology on the other hand. We discuss these more general conjectures in Section 8.3.

3. POSITROID COMBINATORICS

In this section, we review some background on the combinatorics of plabic graphs and the associated objects.

3.1. **Bounded affine permutations.** A (k, N)-*bounded affine permutation* [KLS13] is a bijection $f : \mathbb{Z} \to \mathbb{Z}$ such that

- f is N-*periodic*: $f(i + N) = f(i) + N$ for all $i \in \mathbb{Z}$,
- $i \leq f(i) \leq i + N$ for all $i \in \mathbb{Z}$, and
- $\sum_{i=1}^{N} (f(i) - i) = kN$.

The set of (k, N)-bounded affine permutations is denoted $\text{Bound}(k, N)$. Each $f \in \text{Bound}(k, N)$ gives rise to a unique permutation $\bar{f} \in S_N$ defined by $\bar{f}(i) \equiv f(i) \pmod{N}$ for each $i \in [N]$. Given $f \in \text{Bound}(k, N)$, an integer $i \in \mathbb{Z}$ is called a *loop* (resp., a *coloop*) of f if $f(i) = i$ (resp., $f(i) = i + N$). Thus, $\bar{f}$ has no fixed points if and only if f has no loops and no coloops. In this case, f is uniquely determined by $\bar{f}$, and the integer k is recovered from $\bar{f}$ as follows:

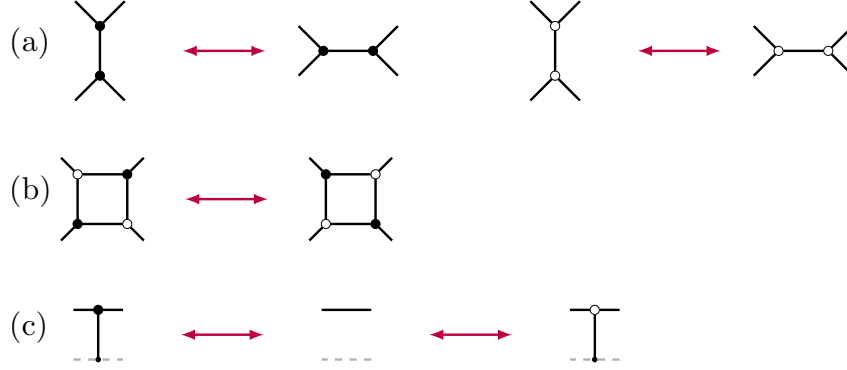$$k = k(\bar{f}) := \#\{i \in [N] \mid \bar{f}(i) < i\}.$$

FIGURE 11. Local moves for plabic graphs: (a) contraction-uncontraction move; (b) square move; (c) tail addition/removal.

We define $\tau_{k,N} \in \mathrm{Bound}(k, N)$ by

$$\tau_{k,N}(i) = \begin{cases} i, & \text{if } 1 \leq i \leq N - k, \\ i + N, & \text{if } N - k + 1 \leq i \leq N, \end{cases}$$

and extend it to a function $\tau_{k,N} : \mathbb{Z} \to \mathbb{Z}$ by N-periodicity.

Let $Q_{k,N} := \{(v, w) \in S_N \times S_N^{(k)} \mid v \leq w\}$, where $\leq$ denotes the Bruhat order on S_N. Given a permutation $u \in S_N$, we can extend it to an N-periodic map $\tilde{u} : \mathbb{Z} \to \mathbb{Z}$ defined by $\tilde{u}(i) = u(i)$ for $i \in [N]$. For $(v, w) \in Q_{k,N}$, let $f_{v,w} := \tilde{w}\tau_{k,N}\tilde{v}^{-1}$. By [KLS13, Proposition 3.15], the map $(v, w) \mapsto f_{v,w}$ gives a bijection $Q_{k,N} \xrightarrow{\sim} \mathrm{Bound}(k, N)$. Taking the inverse of this map, we obtain the following result, justifying the definition of a Richardson link in Section 2.1.3.

Corollary 3.1. *If $\pi \in S_N$ has no fixed points then it can be uniquely factored as a product $\pi = wv^{-1}$, where $(v, w) \in Q_{k,N}$ and $k = k(\pi)$.*

The top-dimensional open positroid variety corresponds to the bounded affine permutation $f_{k,N} \in \mathrm{Bound}(k, N)$ sending $i \mapsto i + k$ for all $i \in \mathbb{Z}$. We let $\pi_{k,N} \in S_N$ be the permutation sending $i \mapsto i + k$ modulo N for all $i \in [N]$.

3.2. **Plabic graphs.** Let G be a plabic graph. Recall from Section 2.1.4 that G must be nonempty, that the boundary vertices of G are labeled by $1, 2, \ldots, N$ in clockwise order, and that the strand permutation $\pi_G : [N] \to [N]$ sends $i \mapsto j$ whenever the strand starting at i terminates at j. We always assume that our plabic graphs G are such that π_G has no fixed points, although most of our constructions can be easily extended to this case.

Definition 3.2 ([Pos06]). We say that G is *reduced* if it has the minimal number of faces among all plabic graphs with strand permutation π_G.

Alternatively [Pos06, Theorem 13.2], a plabic graph G is reduced if and only if G has no closed strands, no self-intersecting strands, and no pairs of strands forming a *bad double crossing* shown in Figure 17(right). *Good double crossings* shown in Figure 17(left) are allowed.

We consider several types of *local moves* on plabic graphs, shown in Figure 11. It was shown in [Pos06] that every permutation $\pi \in S_N$ is the strand permutation of some reduced plabic graph G, and that moreover, any two reduced plabic graphs with the same strand
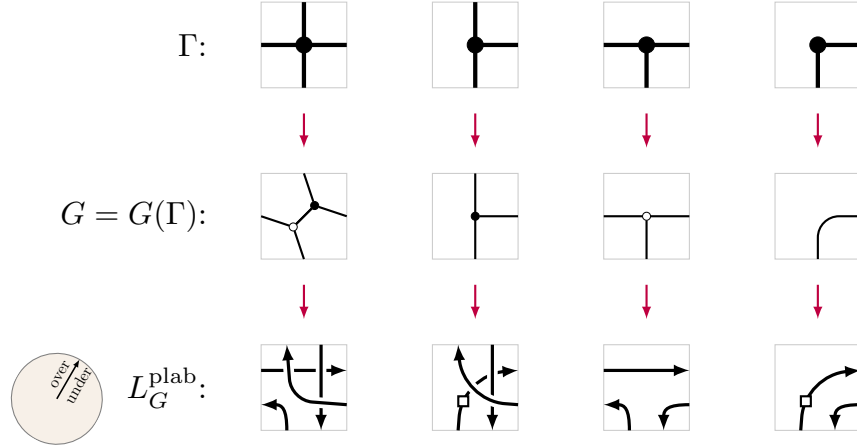
FIGURE 12. Converting a Le-diagram (top row) into a plabic graph (middle row) and into a link (bottom row).

permutation are related by a sequence of the moves (a) and (b) in Figure 11. Below we review one construction of plabic graphs which will be particularly useful to us.

3.3. **Le-diagrams.** Let $\lambda = (\lambda_1 \geq \lambda_2 \geq \cdots \geq \lambda_k \geq 0)$ be a partition, which we identify with its Young diagram. We assume that this Young diagram fits inside a $k \times (N - k)$ rectangle, i.e., satisfies $\lambda_1 \leq N - k$. We draw Young diagrams using *English* (or *matrix*) *notation*. We use matrix coordinates for the boxes of λ, thus, row i contains boxes with coordinates (i, j) for $1 \leq j \leq \lambda_i$, and box $(1, 1)$ is the top left box.

A *Le-diagram* Γ *of shape* λ is a way of placing a dot in some of the boxes of λ so that every box that is below a dot in the same column and to the right of a dot in the same row must also contain a dot. An example of a Le-diagram of shape $\lambda = (3, 3, 3, 1)$ is shown in Figure 15(left). Le-diagrams whose shape fits inside a $k \times (N - k)$ rectangle are in bijection with the elements of $Q_{k,N}$ and $\mathrm{Bound}(k, N)$. Given a Le-diagram Γ of shape λ, one can read off the corresponding pair $(v, w) \in Q_{k,N}$ as follows. First, $w \in S_N^{(k)}$ is the k-Grassmannian permutation corresponding to λ. Specifically, let us label the unit steps in the southeast boundary of λ by $1, 2, \ldots, N$ in increasing order from the northeast to the southwest corner. Then the labels of the vertical steps form a k-element subset of $[N]$, and this set is precisely $\{w(N-k+1), \ldots, w(N)\}$. This determines w uniquely. Alternatively, we can label each box (i, j) of λ with the simple transposition s_{k+j-i}, and then a reduced word for w is obtained by reading these simple transpositions in the northwest direction. Thus, any reduced word for w ends with s_k which labels the box $(1, 1)$. To obtain a reduced word for v, we read these simple transpositions but ignore the ones labeled by dots in Γ. Conversely, given $(v, w) \in Q_{k,N}$, the shape λ of Γ is reconstructed from w, and the empty boxes of Γ correspond to the rightmost subexpression for v inside the (unique up to commutation) reduced word for w.

Example 3.3. For the Le-diagram in Figure 15(left), we have

$$w = s_7 s_3 s_4 s_5 s_6 s_2 s_3 s_4 s_5 s_1 s_2 s_3 s_4 \quad \text{and} \quad v = s_6 s_3 s_2.$$

A Le-diagram Γ can be converted into a plabic graph $G(\Gamma)$ using the local rules shown in the first two rows of Figure 12. This plabic graph is always reduced and has strand permutation $\pi = wv^{-1}$, where $(v, w) \in Q_{k,N}$ are recovered from Γ using the above procedure.
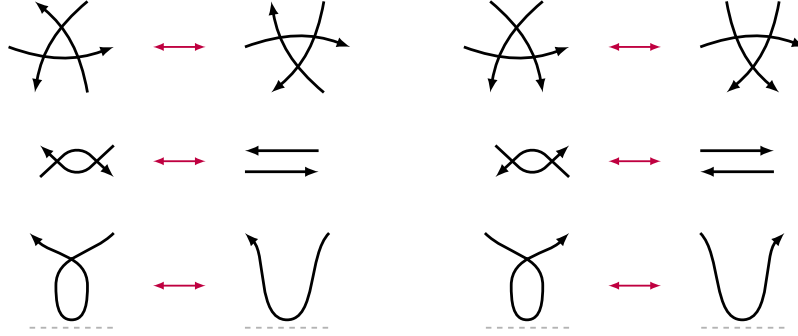
FIGURE 13. Local moves for divides [FPST22, Figures 28–30].

3.4. **Properties of plabic graph links.** Let G be a reduced plabic graph with strand permutation $\pi = \pi_G$. Recall the description of the plabic graph link $L_\pi^{\mathrm{plab}} = L_G^{\mathrm{plab}}$ from Section 2.1.4. It may appear from this description that L_G^{plab} depends on the precise way of drawing the strands in G as smooth curves, or that L_G^{plab} changes if one rotates the graph G (since the over/under-crossings information depends on the complex arguments of the strands). However, it turns out that the link L_G^{plab} is in fact independent of these choices, as explained in [A'C99, STWZ19, FPST22]. Let us give a more invariant description of L_G^{plab}.

Recall that G is embedded in a disk $\mathbf{D} := \{x \in \mathbb{C} : |x| \le 1\}$. Consider the solid torus $\mathbf{D} \times S^1$, and consider an equivalence relation $\sim$ on it defined as follows: for $(x, y), (x', y') \in \mathbf{D} \times S^1$, write $(x, y) \sim (x', y')$ if $x, x' \in \partial\mathbf{D}$ belong to the boundary of the disk and $x = x'$. In other words, we collapse each fiber $x \times S^1$, where $x \in \partial\mathbf{D}$, to a point. The resulting quotient space $\mathbf{D} \times S^1 / \sim$ is homeomorphic to a 3-dimensional sphere S^3.

An *oriented divide* is a smooth immersion of a union of oriented circles (called *branches*) into $\mathbf{D}$. Divides are required to satisfy certain genericity conditions, e.g., that any intersections between the branches must be transversal and belong to the interior of $\mathbf{D}$, and that there have to be no triple intersections; see [FPST22, Definitions 2.1 and 8.1] for a complete list.

Given a branch γ of an oriented divide D, we lift each point of γ to $\mathbf{D} \times S^1$ by letting the S^1 coordinate be the complex argument of the tangent vector of γ at this point. By the genericity assumptions, we obtain an embedding of a union of oriented circles into S^3, i.e., a link, denoted L_D.

The link L_D is invariant under applying the local moves shown in Figure 13 to D; see [FPST22, Proposition 8.4].

Take the strands in our reduced plabic graph G. Each of the N boundary vertices of G has one incoming strand and one outgoing strand. Identifying their endpoints, we obtain an oriented divide $D(G)$. It was shown in [Hir02] that the associated link $L_{D(G)}$ is isotopic to the link L_G^{plab} described in Section 2.1.4. This shows that the link L_G^{plab} is indeed invariant under rotation of G and under small perturbations of the branches of $D(G)$, since this is clearly the case for $L_{D(G)}$.

Remark 3.4. In what follows, it will be convenient to us to use rotational invariance of L_G^{plab}. In our figures, we will fix some angle $\alpha \in [0, 2\pi)$, and assume that the link L_G^{plab} is obtained by first rotating G by the angle $-\alpha$, then applying the description from Section 2.1.4, and then rotating the picture back by α. In other words, if two strands S_1, S_2 in G intersect

at some point p, we consider their complex arguments of tangent vectors in a different interval: $\arg(S_1, p), \arg(S_2, p) \in [\alpha, \alpha + 2\pi)$. Then we draw S_1 above S_2 if and only if $\arg(S_2, p) > \arg(S_1, p)$. And then for all points p where some strand S satisfies $\arg(S, p) = \alpha$, we insert line segments going to the boundary and back. In the figures, the direction α is indicated by the "over/under circle"
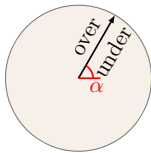
and each point p on a strand S satisfying $\arg(S, p) = \alpha$ is marked by ▫ as in Figure 5.

4. Positroid link isotopies

The goal of this section is to prove Theorem 2.5. We first discuss some properties of plabic graph links, and then we construct a sequence of isotopies, for any permutation $\pi \in S_N$ without fixed points, of the links

$$L_\pi^{\mathrm{Rich}} \cong L_\pi^{\mathrm{plab}} \cong L_\pi^{\mathrm{perm}} \cong L_\pi^{\mathrm{tor}},$$

in that order. When $\pi = \pi_C$ for some concave curve C, we will also show that

$$L_\pi^{\mathrm{tor}} \cong L_\pi^{\mathrm{Cox}},$$

completing the proof.

Throughout this section, we fix a permutation $\pi \in S_N$ without fixed points, and let $(v, w) \in Q_{k,N}$ be the corresponding pair satisfying $\pi = wv^{-1}$, Γ the corresponding Le-diagram of shape λ, and G the corresponding plabic graph, obtained from Γ using the recipe in the first two rows of Figure 12.

4.1. **From Richardson links to plabic graph links.** Our goal is to construct an isotopy between the Richardson link $L_{v,w}^{\mathrm{Rich}}$ (Figure 3(right)) and the plabic graph link L_G^{plab} (Figure 4(c)).

Recall from Remark 2.3 that we are drawing the Richardson braid $\beta_{v,w} = \beta(w) \cdot \beta(v)^{-1}$ in a particular way, so that the crossings of $\beta(w)$ form a shape obtained by rotating λ clockwise by 135°, and the crossings of $\beta(v)^{-1}$ are drawn in some boxes of a shape obtained from the 135°-rotation of λ by reflecting it along the vertical axis; see Figure 3(left). Moreover, the crossings of $\beta(v)^{-1}$ are located precisely in the boxes of λ which do not contain a dot in Γ.

Our first goal is to draw the link $L_{v,w}^{\mathrm{Rich}}$ entirely within λ. To do that, we take $\beta(v)^{-1}$, reflect it along the vertical axis (flipping the over/under-crossings), and place the resulting braid on top of $\beta(w)$. We rotate the result counterclockwise by 135°. Every line segment in the boundary of λ contains an endpoint of a strand in $\beta(v)^{-1}$ and an endpoint of a strand in $\beta(w)$. We join these strand endpoints, obtaining a link diagram drawn inside of λ. This link $L'_{v,w}$, shown in Figure 14, is clearly isotopic to $L_{v,w}$. Intuitively, the transformation $L_{v,w}^{\mathrm{Rich}} \to L'_{v,w}$ can be described as follows: open a book, and place the left (resp., right) half of Figure 3(right) onto the left (resp., right) page of the book. Then close the book with your right hand, so that the front cover of the book is at the bottom. The page containing (the reflection of) $\beta(v)^{-1}$ will be on top of the page containing $\beta(w)$. Finally, rotate the closed book 135° counterclockwise.
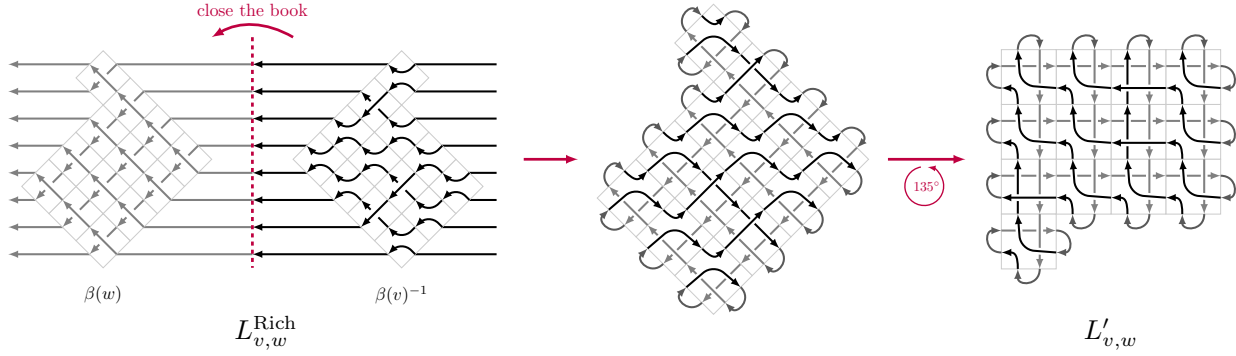
FIGURE 14. Converting the link $L_{v,w}^{\mathrm{Rich}}$ into $L'_{v,w}$; see Section 4.1.
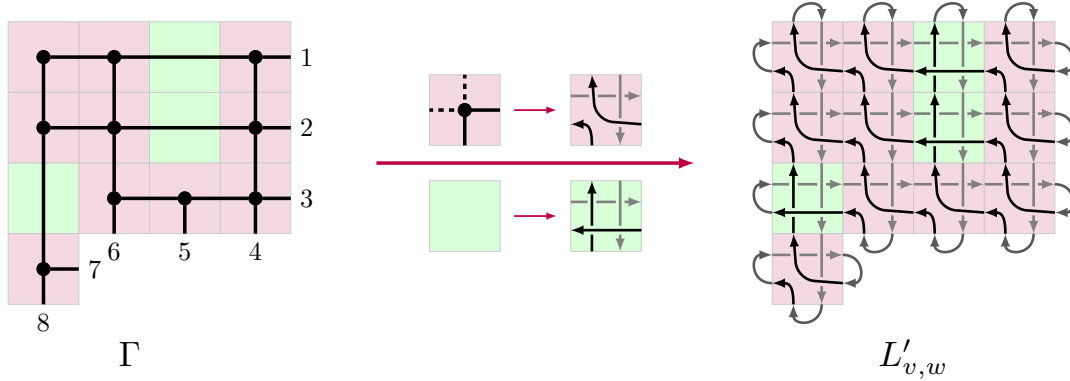

FIGURE 15. Converting a Le-diagram Γ into a link $L'_{v,w}$.

An alternative description of the link $L'_{v,w}$ can be obtained directly from the Le-diagram Γ by replacing each box containing a dot as shown in Figure 15(middle top) and each box not containing a dot as shown in Figure 15(middle bottom). For example, the Le-diagram in Figure 15(left) gets converted into the link $L'_{v,w}$ in Figure 15(right); this is the same link as in Figure 14(right). Since π has no fixed points, each row and each column of Γ contains at least one dot. Consider some column j of Γ and let b_j be the highest box in it which contains a dot. The part of $L'_{v,w}$ above b_j contains a strand going vertically to the top boundary and then back, passing between all the horizontal strands that it encounters along the way. We may therefore contract this piece of the strand to be fully contained inside b_j, as shown in Figure 16(far left). Repeating this procedure for each column $j = 1, 2, \ldots, \lambda_1$, we obtain a link $L''_{v,w}$ isotopic to $L'_{v,w}$; see Figure 16(middle).

Finally, we claim that the link $L''_{v,w}$ is isotopic to the plabic graph link L_G^{plab}. To see this, we choose the angle α from Remark 3.4 to be $80°$. Then combining the rules from Figure 12 for converting the Le-diagram Γ into the plabic graph G with the description of L_G^{plab} given in Section 3.4, we see that a planar diagram of L_G^{plab} is obtained from Γ via the rules shown in the last two rows of Figure 12. Replacing each square (where $\arg(S, p) = \alpha$) by a horizontal segment going to the left boundary above all other strands and back below all other strands, we see that $L_G^{\mathrm{plab}} = L''_{v,w}$; see Figure 16(far right). To summarize, we have constructed explicit isotopies

$$L_\pi^{\mathrm{Rich}} = L_{v,w}^{\mathrm{Rich}} \cong L'_{v,w} \cong L''_{v,w} = L_G^{\mathrm{plab}}.$$
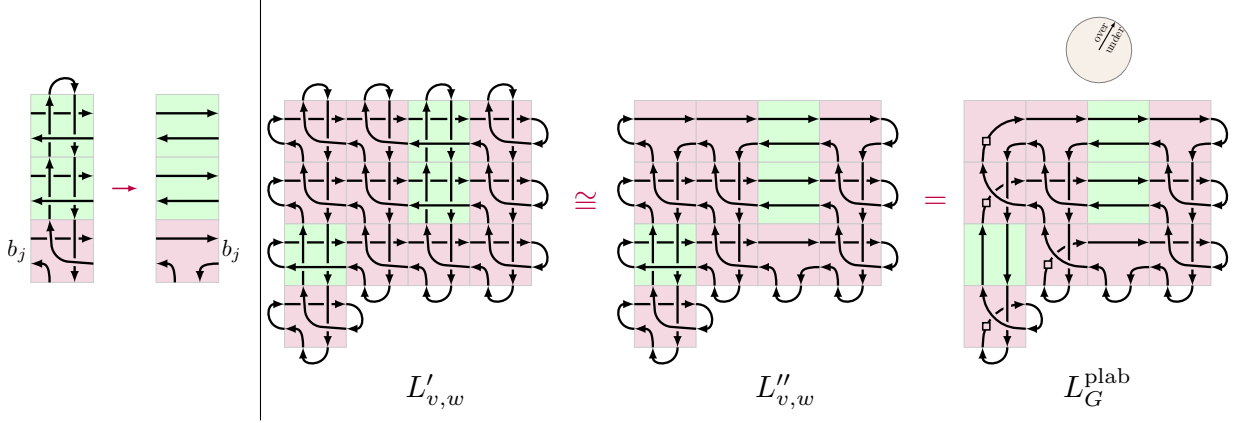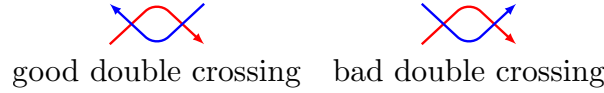
FIGURE 16.   An isotopy from $L'_{v,w}$ to L_G^{plab}.

good double crossing   bad double crossing

FIGURE 17.   Good and bad double crossings of strands in plabic graphs.

4.2. **From plabic graph links to permutation links.** Our goal is to find an isotopy $L_G^{\mathrm{plab}} \cong L_\pi^{\mathrm{perm}}$. Let $D = D(G)$ be the oriented divide obtained from G as in Section 3.4. Let $1, 2, \dots, N$ be the boundary vertices of G. Since G contains no bad double crossings shown in Figure 17(right), it is clear that applying the moves from Figure 13, one can transform D into an oriented divide D' obtained by drawing a straight arrow $i \to \pi(i)$ for each $i \in [N]$. The moves from Figure 13 give rise to link isotopies, so $L_D \cong L_{D'}$. Let us move the boundary vertices $1, 2, \dots, N$ smoothly to the points $1', 2', \dots, N'$ which are located clockwise on the left semicircle of $\partial \mathbf{D}$, i.e., on the subset of $\partial \mathbf{D}$ with negative real part. Let D'' be the oriented divide obtained by drawing a straight arrow $i' \to \pi(i)'$ for each $i \in [N]$. It follows that $L_{D'} \cong L_{D''}$. Let $i, j \in [N]$ be such that the corresponding arrows $S_i := (i' \to \pi(i)')$ and $S_j := (j' \to \pi(j)')$ of D'' cross at some point p. Consider the arguments of the tangent vectors $0 \leq \arg(S_i, p) \neq \arg(S_j, p) < 2\pi$. Then it is easy to check that $\arg(S_i, p) > \arg(S_j, p)$ if and only if $\pi(i) < \pi(j)$. Comparing to the description in Section 2.1.1, we get that $L_{D''} \cong L_\pi^{\mathrm{perm}}$.

4.3. **From permutation links to toric permutation links.** Our goal is to find an isotopy $L_\pi^{\mathrm{perm}} \cong L_\pi^{\mathrm{tor}}$. Recall from Remark 2.2 that L_π^{tor} is isotopic to the *planar grid link* denoted L_π^{grid}; see Figure 2(a–c). In $\tilde{L}_\pi^{\mathrm{grid}}$ and L_π^{grid}, the vertical arrows are drawn above the horizontal arrows.

The main diagonal $y = 1 - x$ of the square $[0,1]^2$ divides L_π^{grid} into the *lower-triangular* and the *upper-triangular* parts. In the lower-triangular part, all vertical arrows point down and all horizontal arrows point right, while in the upper-triangular part, all vertical arrows point up and all horizontal arrows point left. Let us take the lower-triangular part and reflect it around the main diagonal, placing it below the upper-triangular part; see Figure 2(c–d). We obtain a planar diagram of a link which we denote L'_π. Clearly, $L'_\pi \cong L_\pi^{\mathrm{grid}}$. The diagram of L'_π contains arrows pointing, up, left, down, and right. It follows that the over/under-crossings rule in L'_π is given by the following total order on the arrow directions: up > left > down > right. In particular, L'_π is a divide link for the angle $\alpha = 45°$ from Remark 3.4
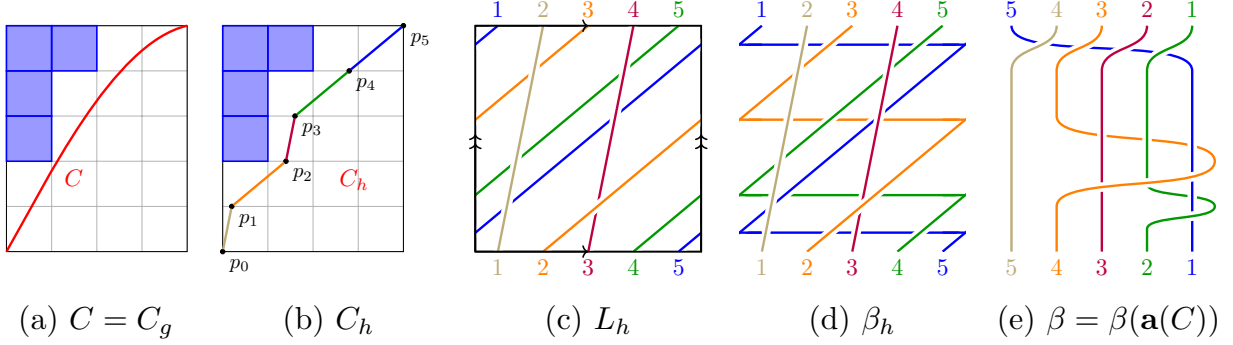
FIGURE 18. Converting a concave curve C into the Coxeter link $\beta(\mathbf{a}(C))$; see Section 4.4.

(where the main diagonal is treated as part of the boundary of the disk), and we get that $L'_\pi \cong L_\pi^{\mathrm{perm}}$.

4.4. From toric permutation links to Coxeter links.

First, we introduce a more general class of links, associated to arbitrary curves inside the $k \times (N - k)$ rectangle.

We say that C_g is a *monotone curve* if it is the plot of a strictly monotone increasing function $g(x) : [0, N - k] \to [0, k]$ satisfying $g(0) = 0$, $g(N - k) = k$, and $g(j) \notin \mathbb{Z}$ for all $j = 1, 2, \ldots, N - k - 1$. Thus, the curve C_g passes through the points $(0, 0)$ and $(N - k, k)$, but through no other lattice points. To any monotone curve C_g we associate a link L_g drawn on the surface of $\mathbb{T}$. The planar diagram of L_g is obtained from the projection $\overline{C}_g$ of C_g to $\mathbb{T}$ via the following rule: whenever two points $(x, g(x))$, $(x', g(x'))$ on C_g (with $x < x'$) project to the same point of $\overline{C}_g$, we draw the projection of $(x, g(x))$ above the projection of $(x', g(x'))$.

The link diagram of L_g is drawn on the torus $\mathbb{T}$, and therefore it is natural to think of L_g itself as a link inside the *thickened torus* $\mathbb{T} \times [0, 1]$. Given a point $p = (x, g(x)) \in C_g$, we denote by $\overline{p} \in \mathbb{T}$ the projection of p to $\mathbb{T}$, and we let $\left(\overline{p}, 1 - \frac{x}{N-k}\right)$ be the corresponding point in $\mathbb{T} \times [0, 1]$. This yields an embedding of C_g into $\mathbb{T} \times [0, 1]$. Under this embedding, the points $(0, 0)$ and $(N - k, k)$ map to $((0, 0), 1)$ and $((0, 0), 0)$, respectively. Adding a line segment connecting $((0, 0), 1)$ to $((0, 0), 0)$, we obtain a representation of the link L_g inside $\mathbb{T} \times [0, 1]$. An obvious consequence of this construction is that the link L_g only depends on the set of lattice points below the plot of g.

Corollary 4.1. *Let C_g, C_h be two monotone curves, and assume that for each $j = 1, 2, \ldots, N - k - 1$, we have $\lfloor g(j) \rfloor = \lfloor h(j) \rfloor$. Then the links L_g and L_h are isotopic.*

Suppose now that $\pi = \pi_C$ for a concave curve C. Our goal is to find an isotopy $L_\pi^{\mathrm{tor}} \cong L_C^{\mathrm{Cox}}$. Comparing the above description to the one in Section 2.1.5, we see that when g is the concave down function satisfying $C = C_g$, we have $L_\pi^{\mathrm{tor}} \cong L_g$. Our goal is to choose a monotone curve C_h such that $L_g \cong L_h$ by Corollary 4.1, and such that $L_h \cong L_C^{\mathrm{Cox}}$.

Let $\lambda = \lambda_C = (\lambda_1 \geq \lambda_2 \geq \cdots \geq \lambda_k = 0)$ be the Young diagram above C. For $r = 0, 1, \ldots, k - 1$, let $p_r := \left(\lambda_{k-r} + \frac{r}{k}, r\right)$. Thus, $p_0 = (0, 0)$. Let $p_k := (N - k, k)$. Let h be the piecewise-linear function whose plot passes through the points $p_0, p_1, \ldots, p_k$, and let C_h be the corresponding monotone curve; see Figure 18(b). Indeed, by Corollary 4.1, we have $L_g \cong L_h$. It remains to establish the isotopy $L_h \cong L_C^{\mathrm{Cox}}$.

Let $\beta = \beta(\mathbf{a}(C))$ be the Coxeter braid associated to C, defined in (2.2). It is a braid on k strands. For $i = 1, 2, \ldots, k$, let $S_i(\beta)$ be the strand of β whose left endpoint is labeled by i. Thus, the right endpoint of $S_i(\beta)$ is labeled by $i + 1$ for $i < k$ and by 1 for $i = k$. On the other hand, the link diagram of L_h in $\mathbb{T}$ intersects the line $y = 0$ in exactly k points with coordinates $\frac{r}{k}$ for $r = 0, 1, \ldots, k - 1$. We would like to view L_h as the closure of a k-strand braid β_h in the solid torus; see Figure 18(c–d). The braid β_h is obtained from L_h via the following procedure: whenever a strand of L_h passes through some point $(1, y) \in [0, 1]^2$ and continues from the point $(0, y) \in [0, 1]^2$, we connect the points $(0, y)$ and $(1, y)$ by a line segment that is drawn below all strands of L_h. The result is a drawing of a braid connecting k points at the bottom of $[0, 1]^2$ to k points at the top of $[0, 1]^2$.

For $i = 1, 2, \ldots, k - 1$, let $S_i(\beta_h)$ be the piece of β_h connecting the point $(\frac{i-1}{k}, 0)$ to the point $(\frac{i}{k}, 1)$. For $i = k$, let $S_k(\beta_h)$ be the remaining piece of β_h, connecting $(\frac{k-1}{k}, 0)$ to $(0, 1)$. See Figure 18(d–e).

We claim that the braids β_h and β are isotopic. We compare them strand-by-strand, identifying $S_i(\beta)$ with $S_{k+1-i}(\beta_h)$ for $i = 1, 2, \ldots, k$, in that order. (This correspondence is indicated via colors in Figure 18(d–e).) For convenience, we rotate the drawing of β 90° counterclockwise. The strand $S_1(\beta)$ moves straight up during the $\ell_2^{a_2} \cdots \ell_k^{a_k}$ part, and then it moves left under all other strands. We apply an isotopy to make $S_k(\beta_h)$ move straight up towards the top boundary of $[0, 1]^2$, and then move left under all other strands. Recall that we have a sequence $\mathbf{a}(C) = (a_2, \ldots, a_k)$ given by $a_i = \lambda_{i-1} - \lambda_i$ for $i = 2, \ldots, k$. Thus, the strand $S_2(\beta)$ wraps around $S_1(\beta)$ exactly a_2 times. On the other hand, $S_{k-1}(\beta_h)$ is the projection to $\mathbb{T}$ of the line segment of C_h connecting p_{k-1} to p_k. This projection intersects the vertical boundary of $\mathbb{T}$ exactly a_2 times. Therefore $S_{k-1}(\beta_h)$ wraps around $S_k(\beta_h)$ exactly a_2 times. Continuing in this fashion, we see that for $i = 3, \ldots, k$, the strand $S_i(\beta)$ wraps around the union $S_1(\beta) \cup S_2(\beta) \cup \cdots \cup S_{i-1}(\beta)$ exactly a_i times. On the other hand, the strand $S_{k+1-i}(\beta_h)$ wraps around the union $S_k(\beta_h) \cup S_{k-1}(\beta) \cup \cdots \cup S_{k+2-i}$ exactly a_i times. This shows that the braids β and β_h are isotopic, and therefore we get an isotopy $L_C^{\mathrm{Cox}} \cong L_h$ between their closures.

5. QUIVERS

In this section, we introduce the point count polynomial $R(Q; q)$ of a locally acyclic quiver, and study its basic properties. We use this polynomial to define the *Q-Catalan number* of Q, an integer that we conjecture to be nonnegative in Conjecture 5.10.

5.1. **Quiver mutation.** Recall that a *quiver* is a directed graph without directed cycles of length 1 and 2.

Given a quiver Q and a vertex $j \in V(Q)$, one can define another quiver $Q' = \mu_j(Q)$ called the *mutation of Q at j*. This operation preserves the set of vertices: $V(Q') = V(Q)$, and changes the set of arrows as follows:

- for every length 2 directed path $i \to j \to k$ in Q, add an arrow $i \to k$ to Q';
- reverse all arrows in Q incident to j;
- remove all directed 2-cycles in the resulting directed graph, one by one.

An *ice quiver* is a quiver $\widetilde{Q}$ whose vertex set $\widetilde{V} = V(\widetilde{Q})$ is partitioned into *frozen* and *mutable* vertices: $\widetilde{V} = V_{\mathrm{fro}} \sqcup V_{\mathrm{mut}}$. We automatically omit all arrows in $\widetilde{Q}$ both of whose endpoints are frozen. For an ice quiver $\widetilde{Q}$, its *mutable part* is the induced subquiver of $\widetilde{Q}$ with vertex set V_{mut}. For a set $S \subset V_{\mathrm{mut}}$, let $\widetilde{Q}[S]$ denote the ice quiver obtained from $\widetilde{Q}$ by

further declaring all vertices in S to be frozen. We write $\widetilde{Q} - S$ for the ice quiver obtained from $\widetilde{Q}$ by removing the vertices in S. For a simply-laced Dynkin diagram D, we say that Q or $\widetilde{Q}$ has type D, or is a D-quiver, if the underlying graph of Q is isomorphic to D.

Let $\widetilde{Q}$ be an ice quiver with $\widetilde{V} = [n + m]$, $V_{\mathrm{mut}} = [n]$, and $V_{\mathrm{fro}} = [n + 1, n + m] := \{n+1, n+2, \ldots, n+m\}$. We represent it by an $(n+m) \times n$ *exchange matrix* $\widetilde{B}(\widetilde{Q}) = (b_{ij})$, defined by

$$b_{ij} = \#\{\text{arrows } i \to j \text{ in } \widetilde{Q}\} - \#\{\text{arrows } j \to i \text{ in } \widetilde{Q}\}.$$

The top $n \times n$ submatrix $B(Q)$ of $\widetilde{B}(\widetilde{Q})$ is skew-symmetric, and is called the *principal part* of $\widetilde{B}(\widetilde{Q})$.

Let $\widetilde{B}$ be an $(n+m) \times n$ matrix. We denote $\mathrm{corank}(\widetilde{B}) := n - \mathrm{rank}(\widetilde{B})$. Following [LS22], we say that an $(n+m) \times n$ matrix $\widetilde{B}$ is *really full rank* if the rows of $\widetilde{B}$ span $\mathbb{Z}^n$ over $\mathbb{Z}$. We say that $\widetilde{Q}$ is *really full rank* if $\widetilde{B}(\widetilde{Q})$ is really full rank, and write $\mathrm{corank}(\widetilde{Q}) := \mathrm{corank}(\widetilde{B}(\widetilde{Q}))$. We say that $\widetilde{Q}$ is *torsion-free* if the abelian group $\mathbb{Z}^{n+m}/\widetilde{B}(\widetilde{Q})\mathbb{Z}^n$ is torsion-free, equivalently, if $\mathbb{Z}^n/\widetilde{B}(\widetilde{Q})^T\mathbb{Z}^{n+m}$ is torsion-free. Thus, $\widetilde{Q}$ is really full rank if and only if it is both full rank and torsion-free.

Definition 5.1. Given a quiver Q, we say that an ice quiver $\widetilde{Q}$ with mutable part Q is a *minimal extension* of Q if $\widetilde{Q}$ has $m = \mathrm{corank}(Q)$ frozen vertices and is really full rank.

Lemma 5.2. *If Q is torsion-free then it admits a minimal extension.*

Proof. If Q is torsion-free, we can find vectors $d_1, \ldots, d_m \in \mathbb{Z}^n$ that form a basis of $\mathbb{Z}^n/B(Q)^T\mathbb{Z}^n$. Define $\widetilde{Q}$ with m frozen vertices so that the bottom m rows of the exchange matrix $\widetilde{B}$ are equal to $d_1, \ldots, d_m$. $\square$

Example 5.3. The exchange matrices of the two quivers Q, Q' in Figure 19(c) are given by

$$B(Q) = \begin{pmatrix} 0 & 2 & -2 \\ -2 & 0 & 2 \\ 2 & -2 & 0 \end{pmatrix} \quad \text{and} \quad B(Q') = \begin{pmatrix} 0 & -1 & -1 & 2 \\ 1 & 0 & 1 & -1 \\ 1 & -1 & 0 & -1 \\ -2 & 1 & 1 & 0 \end{pmatrix}.$$

Thus, $\mathrm{corank}(Q) = 1$, $\mathrm{corank}(Q') = 0$, and neither quiver is torsion-free.

We say that an ice quiver $\widetilde{Q}$ is *isolated* if it has no arrows. For example, the quiver in Figure 8(c) is isolated.

We call an ice quiver $\widetilde{Q}$ *acyclic* if it has no directed cycles, and *mutation acyclic* if it is mutation equivalent to an acyclic ice quiver. For example, any quiver of Dynkin type is acyclic, as is the quiver in Figure 19(a). The quiver in Figure 8(a) and the left quiver in Figure 19(b) are not acyclic, but they are both mutation acyclic.

An edge $u \to v$ in a quiver Q is called a *separating edge* [Mul13] if it does not belong to a bi-infinite walk in Q. Here, a *bi-infinite walk* is a sequence $(w_j)_{j \in \mathbb{Z}}$ of vertices in Q such that for each $j \in \mathbb{Z}$, Q contains an arrow $w_j \to w_{j+1}$.

We define the class of *locally acyclic quivers*, called "Louise" in [MS16, LS22], as follows.

- Any isolated quiver Q is locally acyclic.
- Any quiver that is mutation equivalent to a locally acyclic quiver is locally acyclic.
- Suppose that a quiver Q has a separating edge $u \to v$, and that all three quivers $Q - \{u\}$, $Q - \{v\}$, $Q - \{u, v\}$ are locally acyclic. Then Q is locally acyclic.
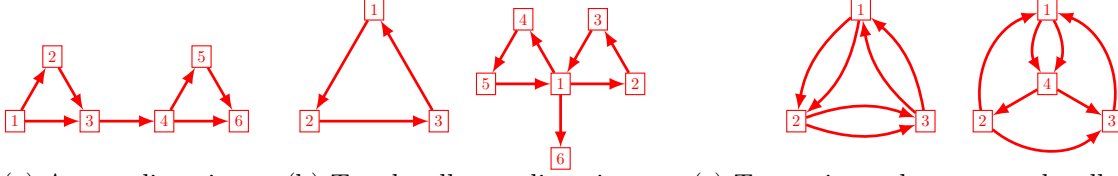
(a) An acyclic quiver   (b) Two locally acyclic quivers.   (c) Two quivers that are not locally acyclic.

FIGURE 19. Acyclic, locally acyclic and non-locally acyclic quivers.

We say that an ice quiver $\widetilde{Q}$ is *locally acyclic* if its mutable part Q is locally acyclic. See Figure 19.

5.2. **Cluster algebras.** Let $\widetilde{Q}$ be an ice quiver with $\widetilde{V} = [n+m]$, $V_{\mathrm{mut}} = [n]$, and $V_{\mathrm{fro}} = [n+1, n+m]$. We associate to $\widetilde{Q}$ the initial seed $(x_1, x_2, \ldots, x_{n+m})$ of *cluster variables*, considered as elements in the function field $\mathcal{F} = \mathbb{Q}(x_1, x_2, \ldots, x_{n+m})$. The variables $x_{n+1}, \ldots, x_{n+m}$ are called *frozen variables*. For a mutation $Q' = \mu_j(Q)$, we associate the seed $(x'_1, x'_2, \ldots, x'_{n+m})$, where $x'_i = x_i$ if $i \neq j$ and one has the new cluster variable

$$x'_j = \frac{\prod_{r \to j} x_r + \prod_{j \to s} x_s}{x_j} \in \mathcal{F}.$$

By repeatedly mutating, we generate (possibly infinitely) many seeds and cluster variables. We denote by $\mathcal{A}(\widetilde{Q}) = \mathcal{A}(\widetilde{B}(\widetilde{Q}))$ the cluster algebra associated to $\widetilde{Q}$. This is the $\mathbb{Z}$-subalgebra of $\mathbb{Q}(x_1, x_2, \ldots, x_{n+m})$ generated by all cluster variables and the inverses of frozen variables.

The *cluster variety* $\mathcal{X}(\widetilde{Q}) = \mathcal{X}(\widetilde{B}(\widetilde{Q}))$ is defined to be the scheme

$$\mathcal{X}(\widetilde{Q}) := \mathrm{Spec}(\mathcal{A}(\widetilde{Q})).$$

We say that $\mathcal{A}(\widetilde{Q})$ (resp., $\mathcal{X}(\widetilde{Q})$) is a cluster algebra (resp., cluster variety) *of type Q*, where Q is the mutable part of $\widetilde{Q}$. We say that $\mathcal{A}(\widetilde{Q})$ is isolated, acyclic, (really) full rank, if $\widetilde{Q}$ is isolated, mutation acyclic, (really) full rank, respectively. If $\widetilde{Q}$ is a locally acyclic quiver, then $\mathcal{A}(\widetilde{Q})$ is locally acyclic in the sense of Muller [Mul13].

Proposition 5.4 ([Mul13, Theorem 7.7], [LS22, Theorem 10.1]). *Suppose that $\widetilde{Q}$ is locally acyclic and really full rank. Then $\mathcal{X}(\widetilde{Q})_{\mathbb{C}}$ is a smooth complex algebraic variety and $\mathcal{X}(\widetilde{Q})_{\bar{\mathbb{F}}_q}$ is smooth for any prime power q.*

Proposition 5.5 ([Mul13, Corollary 5.4]). *Let $i \to j$ be a separating edge in $\widetilde{Q}$. Then the open sets $\{x_i \neq 0\}$ and $\{x_j \neq 0\}$ cover $\mathcal{X}(\widetilde{Q})$.*

Proposition 5.6 ([Mul13, Proposition 3.1, Lemma 3.4, Theorem 4.1]). *Suppose that $i \in V(\widetilde{Q})$ is a mutable vertex such that $Q - \{i\}$ is locally acyclic. Then $\mathcal{A}(\widetilde{Q})[x_i^{-1}] \simeq \mathcal{A}(\widetilde{Q}[i])$.*

5.3. **Quiver point count.** For a mutable quiver Q, we define the function $R(Q; q)$ as follows. Choose a really full rank ice quiver $\widetilde{Q}$ with mutable part Q and m frozen vertices. Then for q a prime power, we set

(5.1) $$R(Q; q) := \frac{\#\mathcal{X}(\widetilde{Q})(\mathbb{F}_q)}{(q-1)^m}.$$

For a rational function $R(q) = P(q)/Q(q)$, we let the *degree* $\deg(R)$ be the difference $\deg(P) - \deg(Q)$.

Proposition 5.7 ([LS22, Proposition 5.11 and Theorem 10.5]). *Let Q be a quiver with n vertices.*

(1) The function $R(Q; q)$ defined in (5.1) does not depend on the choice of $\widetilde{Q}$.

(2) Suppose Q is locally acyclic. Then $R(Q; q)$ is a rational function in q of degree n.

If $u \to v$ is a separating edge in Q and $Q - \{u\}, Q - \{v\}, Q - \{u, v\}$ are locally acyclic, then we have the recurrence

$$(5.2) \quad R(Q; q) = (q - 1)R(Q - \{u\}; q) + (q - 1)R(Q - \{v\}; q) - (q - 1)^2 R(Q - \{u, v\}; q),$$

which follows from Propositions 5.5 and 5.6.

Proposition 5.8 ([LS21, Proposition 3.9]). *Let Q be an acyclic quiver with n vertices. Then*

$$R(Q; q) = \sum_{k \geq 0} a_k (q - 1)^{n-2k} q^k,$$

where a_k is the number of independent sets of size k in the underlying undirected graph of Q.

When Q itself is really full rank, $R(Q; q)$ is a polynomial in q. However, $R(Q; q)$ is in general a genuine rational function whose denominator is a power of $(q - 1)$. E.g., for Q a single isolated vertex (we denote this quiver by A_1; it has corank 1), we have

$$(5.3) \qquad\qquad R(A_1; q) = \frac{q^2 - q + 1}{q - 1}.$$

For an ice quiver $\widetilde{Q}$ with mutable part Q and m frozen vertices, we set

$$R(\widetilde{Q}; q) := (q - 1)^m R(Q; q).$$

Thus, when $\widetilde{Q}$ is really full rank and locally acyclic, $R(\widetilde{Q}; q)$ is a polynomial in q of degree $n + m$ satisfying $\#\mathcal{X}(\widetilde{Q})(\mathbb{F}_q) = R(\widetilde{Q}; q)$ for all prime powers q.

Definition 5.9. Let Q be a torsion-free quiver, and $\widetilde{Q}$ be a minimal extension as in Lemma 5.2. If $R(\widetilde{Q}; q)$ is a polynomial in q, define

$$\chi_Q := R(\widetilde{Q}; 1).$$

By Proposition 5.7, χ_Q does not depend on the choice of $\widetilde{Q}$.

We call χ_Q the *Catalan number* of the quiver Q, or simply the *Q-Catalan number*.

Conjecture 5.10. *Suppose that Q is a locally acyclic quiver. Then $\chi_Q \geq 0$.*

We note that χ_Q can be zero. For example, let Q be an acyclic orientation of the three-cycle, and let $\widetilde{Q}$ be a minimal extension. Thus, $\widetilde{Q}$ is a really full rank quiver with $\text{corank}(Q) = 1$ frozen vertices. Then by Proposition 5.8, we have $R(Q; q) = (q - 1)^3 + 3(q - 1)q$, and thus $R(\widetilde{Q}; q) = (q - 1)^4 + 3(q - 1)^2 q$ and $\chi_Q = 0$. For another example, the quiver Q in Figure 19(a) satisfies $\text{corank}(Q) = 0$ and $\chi_Q = 0$.

Example 5.11. In Table 1, which can be computed using Proposition 5.8 or Corollary 5.15, we take Q to be any orientation of a Dynkin diagram and $\widetilde{Q}$ to be any minimal extension of Q. Note that $R(Q; q) = R(\widetilde{Q}; q)/(q - 1)^m$, where $m = \text{corank}(Q)$ is given in Table 1.

The corresponding HOMFLY polynomials are computed via the following observation, which amounts to a single application of (2.3). Let G be a connected simple plabic graph

such that $Q := Q_G$ is an orientation of a tree, and let Q' (resp., Q'') be obtained from Q by adjoining a path of length 1 (resp., of length 2) to some vertex of Q. Each of Q' and Q'' is the planar dual of some simple plabic graph, and by Lemma 7.6, the HOMFLY polynomials of the associated links are related by

$$(5.4) \qquad P(L'') = \frac{z}{a} P(L') + \frac{1}{a^2} P(L).$$

For example, we can take (Q'', Q', Q) to be one of (A_n, A_{n-1}, A_{n-2}), (D_n, D_{n-1}, D_{n-2}), (E_6, D_5, A_4), (E_7, E_6, D_5), or (E_8, E_7, E_6). Writing $P(Q)$ in place of $P(L)$ where L is the link corresponding to Q, we find:

$$P(A_0) = 1, \quad P(A_1) = \frac{z + z^{-1}}{a} - \frac{z^{-1}}{a^3}, \quad P(A_n) = \frac{z}{a} P(A_{n-1}) + \frac{1}{a^2} P(A_{n-2}) \quad \text{for } n \geq 2.$$

Here A_0 denotes the empty quiver whose associated link is the unknot; the links corresponding to A_1 and A_2 are the Hopf link and the trefoil knot, respectively; see Figure 9. The above recurrence can be solved explicitly: for each $n \geq 1$, we have

$$P(A_n) = \frac{T_{n+1}(z)}{a^{n-1}} - \frac{T_{n-1}(z)}{a^{n+1}}, \quad \text{where} \quad T_n(z) := \sum_{k=0}^{\lfloor n/2 \rfloor} \binom{n-k}{k} z^{n-2k-1}.$$

Similarly, we find

$$P(D_2) = \left(\frac{z + z^{-1}}{a} - \frac{z^{-1}}{a^3} \right)^2, \quad P(D_3) = P(A_3) = \frac{z^3 + 3z + z^{-1}}{a^3} - \frac{z + z^{-1}}{a^5},$$

$$P(D_n) = \frac{z}{a} P(D_{n-1}) + \frac{1}{a^2} P(D_{n-2}) \quad \text{for } n \geq 4.$$

Here D_2 denotes the quiver consisting of two isolated vertices[4] and the associated link is by definition the connected sum of two Hopf links; cf. Proposition 6.6 and (6.3). We also set $D_3 := A_3$. Finally, having computed $P(A_4)$ and $P(D_5)$, we find

$$P(E_6) = \frac{z^6 + 6z^4 + 10z^2 + 5}{a^6} - \frac{z^4 + 5z^2 + 5}{a^8} + \frac{1}{a^{10}};$$

$$P(E_7) = \frac{z^7 + 7z^5 + 15z^3 + 11z + 2z^{-1}}{a^7} - \frac{z^5 + 6z^3 + 9z + 3z^{-1}}{a^9} + \frac{z + z^{-1}}{a^{11}};$$

$$P(E_8) = \frac{z^8 + 8z^6 + 21z^4 + 21z^2 + 7}{a^8} - \frac{z^6 + 7z^4 + 14z^2 + 8}{a^{10}} + \frac{z^2 + 2}{a^{12}}.$$

Substituting $a := q^{-\frac{1}{2}}$ and $z := q^{\frac{1}{2}} - q^{-\frac{1}{2}}$ into the top a-degree term in the above formulas, one recovers the point count formulas in Table 1, in agreement with Theorem 2.9.

Remark 5.12. Let G be a reduced plabic graph with N boundary vertices such that $\pi_G = \pi_{k,N}$ is the "top cell" permutation defined in Section 3.1. For $(k, N) = (2, N)$, $(3, 6)$, $(3, 7)$, $(3, 8)$, we get the quivers $Q_G = A_{N-3}, D_4, E_6, E_8$ respectively. If $\gcd(k, N) = 1$, then it is shown in [GL20] that $m = 0$ and $\chi_{Q_G} = \frac{1}{N}\binom{N}{k}$ is the $(k, N - k)$ rational Catalan number. Compare with Table 1.

---

[4]One can check that the values for D_2 and D_3 are correct by computing the HOMFLY polynomial directly from the plabic graph links for D_4 and D_5 and then running the recurrence (5.4) backwards.

Dynkin type	m	$R(\widetilde{Q}; q)$	χ_Q
A_n, n even	0	$1 + q^2 + q^4 + \cdots + q^n$	$n/2$
A_n, n odd	1	$1 - q + q^2 - q^3 + q^4 - \cdots + q^{n+1}$	1
D_n, $n \geq 4$ even	2	$(1 - q + q^2 - q^3 + q^4 - \cdots + q^{n+2}) + (-q + q^2 + q^n - q^{n+1})$	1
D_n, $n \geq 5$ odd	1	$(1 + q^2 + q^4 + \cdots + q^{n+1}) - (q + q^n)$	$(n-1)/2$
E_6	0	$1 + q^2 + q^3 + q^4 + q^6$	5
E_7	1	$1 - q + q^2 + q^6 - q^7 + q^8$	2
E_8	0	$1 + q^2 + q^3 + q^4 + q^5 + q^6 + q^8$	7

TABLE 1. Point counts of Dynkin quivers.

5.4. **Leaf recurrence.** Let $i \in V(Q)$ be a leaf vertex of a quiver Q, connected to some other vertex $j \in V(Q)$. We call i a *recurrent leaf* if both quivers $Q - \{i\}$ and $Q - \{i, j\}$ are locally acyclic. This automatically implies that Q itself is locally acyclic.

Proposition 5.13. *Fix a field $\mathbb{F}$, and consider cluster varieties over $\mathbb{F}$. Let $\widetilde{Q}$ be a really full rank ice quiver with m frozen vertices and mutable part Q. Let $i \in V(Q)$ be a recurrent leaf in Q connected to $j \in V(Q)$. Then the subvariety of $\mathcal{X}(\widetilde{Q})$ given by $x_i = 0$ is isomorphic to $\mathbb{F} \times \mathcal{X}(\widetilde{Q}')$, where $\widetilde{Q}'$ is a really full rank quiver with m frozen vertices and mutable part $Q' := Q - \{i, j\}$.*

Proof. Our goal is to construct a quiver $\widetilde{Q}'$ satisfying the above assumptions and an isomorphism

$$(5.5) \qquad \{\boldsymbol{x} \in \mathcal{X}(\widetilde{Q}) \mid x_i = 0\} \cong \mathbb{F} \times \mathcal{X}(Q').$$

By Proposition 5.5, the subvariety of $\mathcal{X}(\widetilde{Q})$ given by $x_i = 0$ is contained inside the subvariety of $\mathcal{X}(\widetilde{Q})$ given by $x_j \neq 0$. The quiver $Q - \{j\}$ is the disjoint union of Q' and a single isolated vertex. By assumption, Q' is locally acyclic and thus so is $Q - \{j\}$. By Proposition 5.6, we have $\mathcal{A}(\widetilde{Q})[x_j^{-1}] \cong \mathcal{A}(\widetilde{Q}[j])$. We therefore find

$$(5.6) \qquad \{\boldsymbol{x} \in \mathcal{X}(\widetilde{Q}) \mid x_i = 0\} \cong \{\boldsymbol{x} \in \mathcal{X}(\widetilde{Q}[j]) \mid x_i = 0\}.$$

Let $A = \mathcal{A}(\widetilde{Q}[j] - \{i\})[x_i^{\pm 1}]$ be obtained from the cluster algebra $\mathcal{A}(\widetilde{Q}[j] - \{i\})$ by adjoining x_i and its inverse. The cluster algebra $\mathcal{A}(\widetilde{Q}[j])$ is isomorphic to the subalgebra of A generated by $\mathcal{A}(\widetilde{Q}[j] - \{i\})$, the cluster variable x_i and the mutation x_i', which is of the form f/x_i where $f \in \mathcal{A}(\widetilde{Q}[j] - \{i\})$.

Let $\mathcal{X}' := \mathcal{X}(\widetilde{Q}[j] - \{i\})$. It follows that

$$(5.7) \qquad \mathcal{X}(\widetilde{Q}[j]) \cong \{((x_i, x_i'), \boldsymbol{x}') \in \mathbb{F}^2 \times \mathcal{X}' \mid x_i x_i' = M + x_j M'\},$$

where M, M' are monomials in the frozen variables of $\widetilde{Q}[j] - \{i\}$. We therefore see that the right-hand side of (5.6) is given by

$$(5.8) \quad \{\boldsymbol{x} \in \mathcal{X}(\widetilde{Q}[j]) \mid x_i = 0\} \cong \{((x_i, x_i'), \boldsymbol{x}') \in \mathbb{F}^2 \times \mathcal{X}' \mid x_i = 0 \text{ and } x_i x_i' = M + x_j M'\}.$$

We see that the variable x_i' is free, and thus the right-hand side of (5.8) is isomorphic the direct product of $\mathbb{F}$ and

$$(5.9) \qquad \left\{ \boldsymbol{x}' \in \mathcal{X}' \;\middle|\; \frac{x_j M'}{M} = -1 \right\}.$$

It remains to show that the locus (5.9) is isomorphic to $\mathcal{X}(\widetilde{Q}')$ for some quiver $\widetilde{Q}'$ satisfying the conditions in Proposition 5.13. By assumption, $\widetilde{B} := \widetilde{B}(\widetilde{Q})$ is really full rank. Thus, there exist integers $(\alpha_k)_{k\in[n+m]}$ such that

$$\sum_k \alpha_k \tilde{b}_k = e_i,$$

where $\tilde{b}_k$ denotes the k-th row of $\widetilde{B}$ and $e_i = (0,\ldots,0,1,0,\ldots,0)$ is the i-th standard basis vector in $\mathbb{Z}^n$.

Since i is a leaf, the row $\tilde{b}_i$ has a single nonzero entry in the j-th column. Let $\widetilde{B}^{(1)}$ be obtained from $\widetilde{B}$ by removing the i-th row and the j-th column.[5] Then we have

$$\sum_{k\neq i} \alpha_k \tilde{b}_k^{(1)} = \bar{e}_i,$$

where $\bar{e}_i$ is the i-th standard basis vector in $\mathbb{Z}^{n-1}$. Moreover, the matrix $\widetilde{B}^{(1)}$ is still really full rank.

Let $V_{\mathrm{fro}} := [n+1, n+m]$ be the set of frozen vertices of $\widetilde{Q}$. Then the set of frozen vertices of $\widetilde{Q}[j] - \{i\}$ is $V_{\mathrm{fro}} \sqcup \{j\}$. We have $\gcd(\alpha_k \mid k \in V_{\mathrm{fro}} \sqcup \{j\}) = 1$ since all the rows with a nonzero entry in column i of $\widetilde{B}$ belong to $V_{\mathrm{fro}} \sqcup \{j\}$. By [LS22, Section 5], replacing a frozen row by its negative, or adding a frozen row to another frozen row produces an isomorphic cluster variety. After applying a series of such transformations, we obtain a really full rank $(n+m-1)\times(n-1)$ exchange matrix $\widetilde{B}^{(2)}$ and a family of integers $(\alpha_k^{(2)})_{k\neq i}$ satisfying

$$(5.10) \qquad\qquad \sum_{k\neq i} \alpha_k^{(2)} \tilde{b}_k^{(2)} = \bar{e}_i,$$

such that moreover for some $\ell \in V_{\mathrm{fro}} \sqcup \{j\}$ we have $\alpha_\ell^{(2)} = 1$.

Now, let $\widetilde{B}^{(3)}$ be the $(n+m-1)\times(n-2)$ matrix obtained from $\widetilde{B}^{(2)}$ by further removing the i-th column. Thus, $\mathcal{A}(\widetilde{B}^{(3)}) \cong \mathcal{A}(\widetilde{Q}[j] - \{i\})$, and by construction, $\sum_{k\neq i} \alpha_k^{(2)} \tilde{b}_k^{(3)} = 0$ is the zero vector in $\mathbb{Z}^{n-2}$. Thus, by [LS22, Proposition 5.1], the numbers $(\alpha_k^{(2)})_{k\neq i}$ describe a one-parameter subgroup $\mathbb{F}^*$ of the cluster automorphism torus $T = \mathrm{Aut}(\mathcal{A}(\widetilde{B}^{(2)}))$ (see [LS22, Section 5]), with $z \in \mathbb{F}^*$ acting by $x_k \mapsto z^{\alpha_k^{(2)}} x_k$. Equation (5.10) implies that z acts on the monomial $\frac{x_j M'}{M}$ by $z^{\pm 1}$. Thus, every $\mathbb{F}^*$-orbit contains a unique point in the locus (5.9). In other words, the locus (5.9) is isomorphic to the quotient $\mathcal{X}(\widetilde{B}^{(2)})/\mathbb{F}^*$. Since we assumed that $\alpha_\ell^{(2)} = 1$, the quotient $\mathcal{X}(\widetilde{B}^{(2)})/\mathbb{F}^*$ can be obtained by setting $x_\ell = 1$. Let $\widetilde{B}'$ be the $(n+m-2)\times(n-2)$ obtained from $\widetilde{B}^{(3)}$ by removing the ℓ-th row. Let $\widetilde{Q}'$ be the associated quiver, with m frozen vertices corresponding to the rows $(V_{\mathrm{fro}} \sqcup \{j\}) \setminus \{\ell\}$ and mutable part $Q - \{i,j\}$. Clearly, $\widetilde{Q}'$ is still really full rank. We find that indeed the locus (5.9) is isomorphic to $\mathcal{X}(\widetilde{Q}')$. □

Remark 5.14. Proposition 5.13 generalizes to the case of i being either a source or a sink in Q.

The following result will be later compared to the HOMFLY skein relation (2.3).

---

[5]When removing rows and columns from matrices, we preserve the labels of the remaining rows and columns. For instance, removing row 1 from $\widetilde{B}$ produces a matrix with rows labeled $2,\ldots,n+m$.
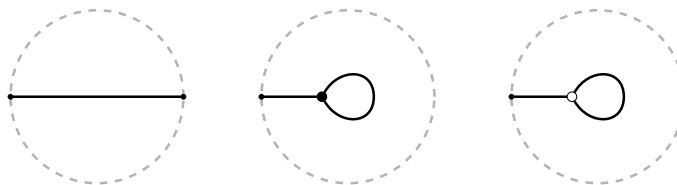
(a) no interior faces   (b) one interior face   (c) one interior face

FIGURE 20. Tail reductions that have boundary vertices.

Corollary 5.15. *Let Q be really full rank, and let $i \in V(Q)$ be a recurrent leaf in Q connected to $j \in V(Q)$. Let $Q' := Q - \{i\}$ and $Q'' := Q - \{i, j\}$. Then*

(5.11) $$R(Q; q) = (q - 1)R(Q'; q) + qR(Q''; q).$$

Proof. Let $\widetilde{Q}$ be really full rank with mutable quiver Q, and $\mathcal{X} := \mathcal{X}(\widetilde{Q})$. Let $\mathcal{U} := \{x_i \neq 0\}$ and $\mathcal{Z} := \{x_i = 0\}$ be two subvarieties of $\mathcal{X}$. Then $\mathcal{U}$ is a really full rank cluster variety of type Q' and $\mathcal{Z}$ is described in Proposition 5.13. The result follows since

$$\#\mathcal{X}(\mathbb{F}_q) = \#\mathcal{U}(\mathbb{F}_q) + \#\mathcal{Z}(\mathbb{F}_q). \qquad \square$$

6. QUIVERS, LINKS, AND PLABIC GRAPHS

In this section, we study some basic relations between the properties of plabic graphs and the associated quivers and links.

6.1. **Plabic graph quivers.** Recall the background on plabic graphs from Sections 2.1.4 and 3.2. We continue to assume that each plabic graph G is trivalent, and that each interior face of G is simply connected.

We say that two plabic graphs are *move equivalent* if they are connected by a sequence of moves in Figure 11. For the square move in Figure 11(b), we require that the four faces A, B, C, D adjacent to the square face in clockwise order satisfy $A \neq B \neq C \neq D \neq A$. (Having $A = C$ or $B = D$ is allowed.) Cf. [FPST22, Restriction 6.3]; this restriction is needed in order for natural statements such as Proposition 6.2 to hold.

Proposition 6.1. *Let G be a connected plabic graph. Then G can be transformed using only tail removal (Figure 11(c)) into:*
- *the graph in Figure 20(a) if G has no interior faces;*
- *the graph in Figure 20(b) or Figure 20(c) if G has one interior face;*
- *a plabic graph with no boundary vertices, if G has two or more interior faces.*

We call this graph the tail reduction *of G.*

Proof. Let G be a connected plabic graph. By repeatedly applying tail removal to G (without changing connectedness or the number of interior faces), we may assume no more tail removals are possible. If G has no boundary vertices then G must have two or more interior faces. If G has a boundary vertex b connected to an interior vertex v, then v must be incident to a loop edge, for otherwise we may apply a tail removal to b. In this case, G has one interior face. Finally, if G has no interior vertices, then G consists of a single edge connecting two boundary vertices, and has no interior faces. $\qquad \square$
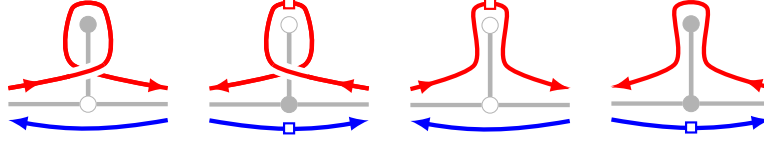
FIGURE 21. The behavior of the link L_G^{plab} at interior leaves.

Proposition 6.2.
- *Suppose that two simple plabic graphs G and G' are move equivalent. Then Q_G and $Q_{G'}$ are mutation equivalent.*
- *Any plabic graph G' move equivalent to a simple plabic graph G is also simple.*

Proof. Direct check. □

Recall from Section 2.2 that each plabic graph gives rise to a link L_G^{plab} and that our main conjecture (Conjecture 2.8) yields a relation between the polynomials $R(Q_G; q)$ and $P(L_G^{\mathrm{plab}}; a, z)$. For a rational function $R(q) = P(q)/Q(q)$, the *leading coefficient* of $R(q)$ is defined as the ratio of the coefficient of $q^{\deg P}$ in $P(q)$ and the coefficient of $q^{\deg Q}$ in $Q(q)$. While Conjecture 2.8 applies only to simple plabic graphs (cf. Section 9.3), the following more basic statement appears to hold for arbitrary plabic graphs. In particular, we allow plabic graphs with interior leaves, though we still insist that interior faces are simply connected. The link L_G^{plab} is defined as before, and the behavior of the strands at an interior leaf is shown in Figure 21.

Conjecture 6.3. *Let G be a plabic graph with $\mathrm{c}(G)$ connected components and n interior faces. Then the top a-degree of $P(L_G^{\mathrm{plab}}; a, z)$ equals*

$$(6.1) \qquad \deg_a^{\mathrm{top}}(P(L_G^{\mathrm{plab}})) = \mathrm{c}(G) - n - 1.$$

The degree of $P^{\mathrm{top}}(L; q)$ (as a rational function in q) is given by

$$(6.2) \qquad \deg(P^{\mathrm{top}}(L; q)) = n,$$

and the leading coefficient of $P^{\mathrm{top}}(L; q)$ is equal to 1.

Cluster varieties $\mathcal{X}(\widetilde{Q})$ are irreducible, with dimension equal to the number of vertices in $\widetilde{Q}$. Thus, when $R(Q; q)$ is a rational function, it has leading coefficient 1 and degree equal to the number of vertices of Q. So Conjecture 2.8 implies (6.2) for simple plabic graphs.

6.2. Empty quivers.

Proposition 6.4. *Let G be a connected plabic graph. The following are equivalent:*
- *(1) Q_G is empty.*
- *(2) G is a tree.*
- *(3) The tail reduction of G is a graph with no interior vertices.*

Proof. The mutable quiver Q_G is empty if and only if G has no interior faces, which is equivalent to G being a tree, since G is assumed to be connected. By Proposition 6.1, this is also equivalent to (3). □
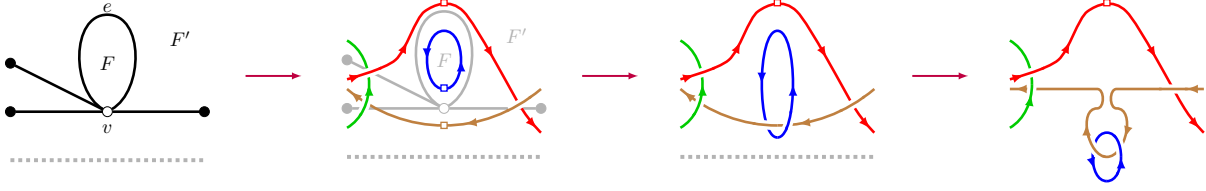
FIGURE 22. A loop edge in G whose sole vertex is adjacent to a boundary face results in having the Hopf link as a connected summand of L_G^{plab}; see the proof of Proposition 6.7.

6.3. **Disconnected graphs.** For two plabic graphs G', G'', we let $G' \sqcup G''$ denote the disconnected plabic graph obtained by taking the disjoint union of G' and G''. We denote by the same symbol the disjoint union of two quivers and of two links.

Proposition 6.5. *Suppose $G = G' \sqcup G''$ is a disconnected plabic graph. Then $Q_G = Q_{G'} \sqcup Q_{G''}$ and $L_G^{\text{plab}} = L_{G'}^{\text{plab}} \sqcup L_{G''}^{\text{plab}}$.*

Proof. Follows directly from the definitions. □

6.4. **Isolated plabic graph quivers.** Recall that the *connected sum* of two oriented knots K, K' is defined as follows. Find planar projections of the two knots that are disjoint. Then find a (topological) rectangle R in the plane, with oriented boundary consisting of sides S_1, S_2, S_3, S_4 in order, such that S_1 (resp. S_3) is an oriented arc along K (resp. K'), and S_2, S_4 are disjoint from K and K'. The oriented connected sum knot $K \# K'$ is obtained by deleting S_1, S_3 and adding S_2, S_4. To construct the connected sum of two links L, L', we choose components $K \subset L$ and $K' \subset L'$ and perform the above surgery. We call any link produced in this way the *connected sum* of L and L', denoted $L \# L'$. The following result is well known; see e.g. [Lic97, Proposition 16.2].

Proposition 6.6. *Let L and L' be two oriented links. Then $P(L \sqcup L') = \left(\frac{a - a^{-1}}{z} \right) P(L) P(L')$ and $P(L \# L') = P(L) P(L')$.*

In particular, the r-component unlink has HOMFLY polynomial $\left(\frac{a - a^{-1}}{z} \right)^{r-1}$.

Let $L_{\text{Hopf}} := $ denote the positively oriented Hopf link. Then we have

$$(6.3) \qquad P(L_{\text{Hopf}}; a, z) = \frac{z + z^{-1}}{a} - \frac{z^{-1}}{a^3}.$$

Recall that a quiver Q is *isolated* if it has no arrows.

Proposition 6.7. *Let G be a simple plabic graph with n interior faces and $c(G)$ connected components. Suppose that Q_G is isolated. Then L_G^{plab} is a disjoint union of $c(G)$ links, each of which is a connected sum of some number (possibly zero) of positively oriented Hopf links.*

Proof. By Proposition 6.5, we may assume that G is connected. Replace G by its tail reduction (Proposition 6.1). Then the result holds when $n = 0$: the link L_G^{plab} is an unknot. The result also holds when $n = 1$: the link L_G^{plab} is the Hopf link. So suppose that $n > 1$. In particular, we are assuming that G has no boundary vertices.
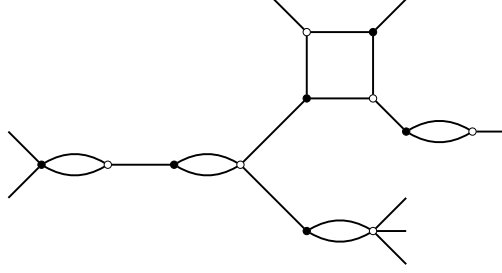
FIGURE 23.   A "tree" of interior faces (without boundary vertices) must have a loop.

For the remainder of the proof it is convenient to replace G by its *bipartite reduction*, obtained by contracting all interior edges whose endpoints have the same color. In particular, interior vertices are allowed to have degree higher than three. Suppose first that G contains an interior face F which is bounded by a loop e whose sole endpoint is $v \in V(G)$. We show that v must be adjacent to a boundary face of G. Without loss of generality, we may assume that the edge e is not fully contained inside any other loop edge incident to v. Let F' be the face on the other side of e to F. If F' is a boundary face then we are done. Otherwise, we assume that F' is an interior face. Let e' be any non-loop edge incident to v that is on the boundary of F'. By our bipartite assumption, e' connects v to a vertex of opposite color. The assumptions that G is simple and Q_G is isolated then imply that e' separates F' from a boundary face. It follows that v is adjacent to a boundary face of G. Letting $L' := L^{\text{plab}}_{G-e}$, we see from Figure 22 that G is a connected sum of L' and L_{Hopf}. Since $G - e$ has fewer interior faces, the result follows by induction.

Suppose now that G, still assumed to be bipartite, has no interior faces that are bounded by loop edges. Let F be an interior face of G. Since G is simple, the perimeter of F does not contain both sides of any edge. Moreover, since Q_G is isolated, every edge adjacent to F is adjacent to a boundary face on the other side. Thus, G consists of a number of interior faces connected in a tree-like manner as in Figure 23. The interior faces at the leaves of this tree must be bounded by loop edges, contradicting our assumption.   □

6.5. **Torsion.** By definition, for G a (possibly not simple) plabic graph, the quiver Q_G^- is obtained from the directed graph Q_G (Section 2.2) by removing all 1-cycles, and canceling out directed 2-cycles one by one. This agrees with the procedure in [FPST22], and the mutation class of Q_G^- is again invariant under the moves in Figure 11. Note that G is simple if and only if $Q_G = Q_G^-$.

Proposition 6.8. *Let G be a plabic graph. Then Q_G^- is torsion-free.*

Proof. We prove the result by induction on the number of vertices of Q_G^-. In the following, we index rows of the $B(Q_G^-)$ by interior faces F of G.

We may suppose that G is connected. If G has fewer than two interior faces, then checking the graphs in Figure 20, we see that the result holds. So suppose that G has at least two interior faces. Applying tail removal, we may suppose that G is not reduced. Then by [Pos06], one of the following holds: (a) G has an interior leaf, or (b) the bipartite reduction (see the proof of Proposition 6.7) has a loop, or (c) G is move equivalent to a plabic graph with a two parallel edges between vertices of opposite color.

In case (a), removing the leaf vertex does not change Q_G^-. We may thus assume that all interior leaves have been removed. In case (b), deleting the loop edge removes a zero row and a zero column from $B(Q_G^-)$, so the result holds by induction. We may thus assume that G is leafless and loopless and we are in situation (c), that is, G has a double edge: a pair e', e'' of edges between vertices u, v of opposite colors. Let F be the interior face between e' and e'', and let F', F'' be the faces on the other side of e' and e'' to F; see Figure 24. Let G' be obtained from G by removing both edges e', e''. Let $B := B(Q_G^-)$, $C := B(Q_{G'}^-)$, and $n := |V(Q_G^-)|$. If F', F'' are both boundary faces, then $Q_{G'}^-$ is obtained from Q_G^- by removing an isolated vertex, so the result holds by induction.

Suppose that one of the faces F', F'' is boundary and one, say F', is interior. Then $Q_{G'}^-$ is obtained from Q_G^- by removing the vertices F and F'. Let $\mathbb{Z}^V \cong \mathbb{Z}^n$ denote the free $\mathbb{Z}$-module with basis vectors $\{e_H\}_{H \in V}$ indexed by the vertex set $V = V(Q_G^-) = \{\text{interior faces } H \text{ of } G\}$ and $\mathbb{Z}^{n-2} \cong \mathbb{Z}^{V'} \subset \mathbb{Z}^V$ the submodule spanned by basis elements other than $e_F, e_{F'}$. The rows of B belong to $\mathbb{Z}^V$ and the rows of C belong to $\mathbb{Z}^{V'} \subset \mathbb{Z}^V$. By induction, C is torsion-free, so $\mathbb{Z}^{V'}/C^T\mathbb{Z}^{V'}$ has a basis given by some vectors $d_1, d_2, \ldots, d_r \in \mathbb{Z}^{V'}$. Furthermore, we have

$$b_F = \pm e_{F'}, \qquad b_{F'} \pm e_F \in \mathbb{Z}^{V'}, \qquad b_H - c_H \in \mathbb{Z}e_{F'},$$

where H is any interior face other than F, F', and b_H and c_H denote the rows of B and C, respectively. It is clear that $\mathbb{Z}^V/B^T\mathbb{Z}^V$ has a basis given by $\{d_1, \ldots, d_r\}$. So B is torsion-free.

Now suppose that F', F'' are both interior faces. If $F' = F''$, then one of u, v, say v, must be a cut vertex of G. Thus, G contains a non-trivial induced subgraph H containing v and connected to $G - H$ only via e', e''. The subgraph H is contained "inside" $F' = F''$; we may consider H to be a plabic graph, necessarily not reduced, with a single boundary vertex incident to v. Replacing G by H and repeating the argument, we are reduced the situation where $F' \neq F''$.

With $F' \neq F''$ both interior, $Q_{G'}^-$ is obtained from Q_G^- by removing the vertex F and identifying the vertices F' and F'' to give a new vertex $\tilde{F}$ of $Q_{G'}^-$. The rows of B belong to $\mathbb{Z}^V \cong \mathbb{Z}^n$ and the rows of C belong to $\mathbb{Z}^{V'} \cong \mathbb{Z}^{n-2}$, where $V' = V(Q_{G'}^-)$. Define the inclusion $\iota : \mathbb{Z}^{V'} \hookrightarrow \mathbb{Z}^V$ by sending $e_{\tilde{F}}$ to $e_{F'}$, and mapping the other basis vectors in the obvious way. By induction, C is torsion-free, so $\mathbb{Z}^{V'}/C^T\mathbb{Z}^{V'}$ has a basis given by some vectors $d_1, d_2, \ldots, d_r \in \mathbb{Z}^{V'}$. We have that

$$b_F = \pm(e_{F'} - e_{F''}), \qquad b_{F'} + b_{F''} = \iota(c_{\tilde{F}}), \qquad b_H - \iota(c_H) \in \mathbb{Z}(e_{F'} - e_{F''}),$$

where H is an interior face other than F, F', F''. Let $W \subset \mathbb{Z}^{V-\{F\}}$ be the span of the vectors $b_F, b_{F'} + b_{F''}$ and $b_H, H \notin \{F, F', F''\}$. Then $\{\iota(d_1), \ldots, \iota(d_r)\}$ form a basis of $\mathbb{Z}^{V-\{F\}}/W$. But $b_{F'} \pm e_F \in \mathbb{Z}^{V-\{F\}}$, so $\mathbb{Z}^V/B^T\mathbb{Z}^V$ has basis $\{\iota(d_1), \ldots, \iota(d_r)\}$. Thus, B is torsion-free. $\qquad \square$

Combining Proposition 6.8 with Lemma 5.2, we obtain the following result.

Corollary 6.9. *Let G be a simple plabic graph. Then Q_G admits a minimal extension.*

7. SKEIN RELATIONS

In this section, we introduce leaf recurrent plabic graphs. This class of plabic graphs includes the well-studied reduced plabic graphs and plabic fences. We show that the leaf recurrence for plabic graphs corresponds to the skein relation for the associated links, thus establishing Conjecture 2.8 for leaf recurrent plabic graphs.
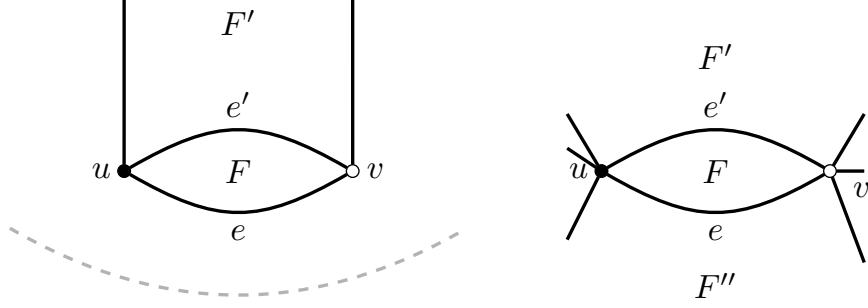
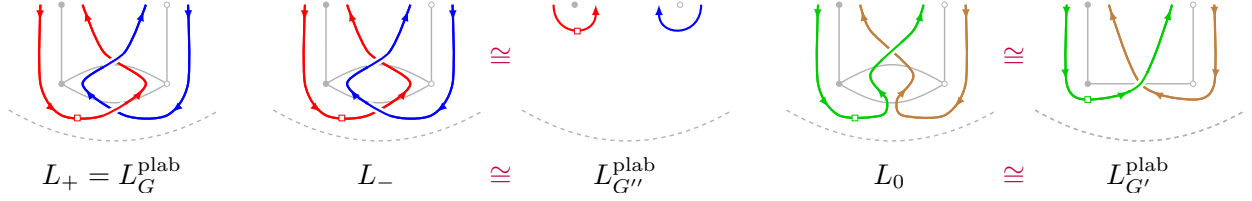FIGURE 24.   A boundary leaf face F (left) and an interior double edge (right).

$$L_+ = L_G^{\text{plab}} \qquad L_- \qquad \cong \qquad L_{G''}^{\text{plab}} \qquad L_0 \qquad \cong \qquad L_{G'}^{\text{plab}}$$

FIGURE 25.   Leaf recurrence for plabic graphs corresponds to the HOMFLY skein relation; see Lemma 7.6.

7.1. **Leaf recurrent plabic graphs.** In this section, we assume that all plabic graphs satisfy the assumptions of Section 6.1.

Definition 7.1. Let G be a plabic graph. An interior face F of G is a *boundary leaf face* if, in the tail reduction of G, the face F has the form shown in Figure 24, i.e., F is bounded by two edges e, e' with endpoints u, v of distinct color, with e separating F from a boundary face and e' separating F from an interior face F'.

Lemma 7.2. *Let G be a simple plabic graph and F a boundary leaf face. Let $u, v \in V(G)$ be the vertices adjacent to F. Then the plabic graphs $G' := G - e$ and $G'' := G - \{u, v\}$ are both simple.*

Proof. The directed graph $Q_{G'}$ is obtained from Q_G by removing the vertex corresponding to F. Similarly, $Q_{G''}$ is obtained from Q_G by removing the vertices corresponding to F and F'. Both directed graphs are clearly quivers, and thus G', G'' are simple.   □

Definition 7.3. The class of *leaf recurrent* plabic graphs is defined as follows.
(a) Every leaf recurrent plabic graph is simple.
(b) If Q_G is isolated then G is leaf recurrent.
(c) If G is move equivalent to a leaf recurrent plabic graph then G is leaf recurrent.
(d) Suppose G has a boundary leaf face F as in Lemma 7.2. If the plabic graphs G' and G'' are leaf recurrent then G is leaf recurrent.

Remark 7.4. It is immediate that if G is leaf recurrent then Q_G is locally acyclic.

Theorem 7.5 ([MS16, Remark 4.7]). *Any reduced plabic graph G is leaf recurrent.*

7.2. **The skein relation.**

Lemma 7.6. *Suppose that G is a plabic graph with a boundary leaf face F. Let $L_+ := L_G^{\mathrm{plab}}$, $L_0 := L_{G'}^{\mathrm{plab}}$, and $L_- := L_{G''}^{\mathrm{plab}}$, where G, G', G'' are the three graphs in Lemma 7.2. Then the HOMFLY polynomials of (L_+, L_0, L_-) are related by (2.3).*

Proof. See Figure 25. □

Theorem 7.7. *Suppose G is a leaf recurrent plabic graph. Then Conjectures 2.8 and 6.3 hold for G.*

Proof. Suppose G has a boundary leaf face F such that the graphs G', G'' from Lemma 7.2 are both leaf recurrent. Denote $Q := Q_G$, $Q' := Q_{G'}$, $Q'' := Q_{G''}$, $L_+ := L_G^{\mathrm{plab}}$, $L_0 := L_{G'}^{\mathrm{plab}}$, and $L_- := L_{G''}^{\mathrm{plab}}$, and note that G, G', G'' all have the same number of connected components.

By Lemma 7.6, the HOMFLY polynomials of (L_+, L_0, L_-) are related by (2.3). By Remark 7.4, the quivers Q, Q', Q'' are locally acyclic. By Corollary 5.15, their point counts are related by (5.11). Comparing (2.3) and (5.11), we see that (2.4) holds for Q if it holds for both Q' and Q''.

Now suppose that Q_G is isolated with n vertices. If G is the disjoint union of G_1 and G_2 then by Proposition 6.6, we have $P(L_G^{\mathrm{plab}}) = ((a - a^{-1})/z)P(L_{G_1}^{\mathrm{plab}})P(L_{G_2}^{\mathrm{plab}})$, so $P^{\mathrm{top}}(L_G^{\mathrm{plab}}; q) = (q-1)^{-1}P^{\mathrm{top}}(L_{G_1}^{\mathrm{plab}}; q)P^{\mathrm{top}}(L_{G_2}^{\mathrm{plab}}; q)$. Since $R(Q_G; q) = R(Q_{G_1}; q)R(Q_{G_2}; q)$, the result follows. We may now assume that G is connected. By Proposition 6.7, L_G^{plab} must be the connected sum of n Hopf links. By Proposition 6.6, (6.3) and (5.3) we have

$$P^{\mathrm{top}}(L_G^{\mathrm{plab}}; q) = \left(\frac{q^2 - q + 1}{q - 1}\right)^n = R(Q_G; q).$$

Thus, the result holds when Q_G is isolated.

Since the validity of (2.4) is unchanged under moves on G, it follows that (2.4) holds for all leaf recurrent plabic graphs G. The equality (6.1) also follows from the same argument. □

7.3. **Plabic fences.** Following [FPST22, Section 12], we consider the following class of plabic graphs. Let $N \geq 2$ and let $I := [N-1] = \{1, 2, \ldots, N-1\}$. A *double braid word* is a word $\mathbf{w} = (i_1, i_2, \ldots, i_m)$ in the alphabet

$$\pm I := \{-1, -2, \ldots, -(N-1)\} \sqcup \{1, 2, \ldots, N-1\}.$$

We denote the set of double braid words of length m by $(\pm I)^m$.

To a double braid word $\mathbf{w} \in (\pm I)^m$ we associate a plabic graph $G(\mathbf{w})$ with $2N$ boundary vertices. First, draw N horizontal strands, with both endpoints of each strand on the boundary of the disk. Then for each $j = 1, 2, \ldots, m$, let $h := |i_j|$ and consider the strands at height h and $h + 1$. If $i_j > 0$, add a black at h, white at $h + 1$ bridge between these two strands, and if $i_j < 0$, add a white at h, black at $h+1$ bridge between these two strands. The bridges are added one by one proceeding from left to right. See Figure 26 for an example.

Proposition 7.8. *For any $\mathbf{w} \in (\pm I)^m$, the plabic graph $G(\mathbf{w})$ is simple.*

Proof. This is clear from construction. □

Let us say that two braid words $\mathbf{w}, \mathbf{w}'$ are *double braid move equivalent* if they are related by a sequence of the following moves:
(B1) $(\ldots, i, j, i, \ldots) \leftrightarrow (\ldots, j, i, j, \ldots)$ if $i, j \in \pm I$ have the same sign and $|i - j| = 1$;
(B2) $(\ldots, i, j, \ldots) \leftrightarrow (\ldots, j, i, \ldots)$ if $i, j \in \pm I$ have the same sign and $|i - j| > 1$;
(B3) $(\ldots, i, j, \ldots) \leftrightarrow (\ldots, j, i, \ldots)$ if $i, j \in \pm I$ have different signs;
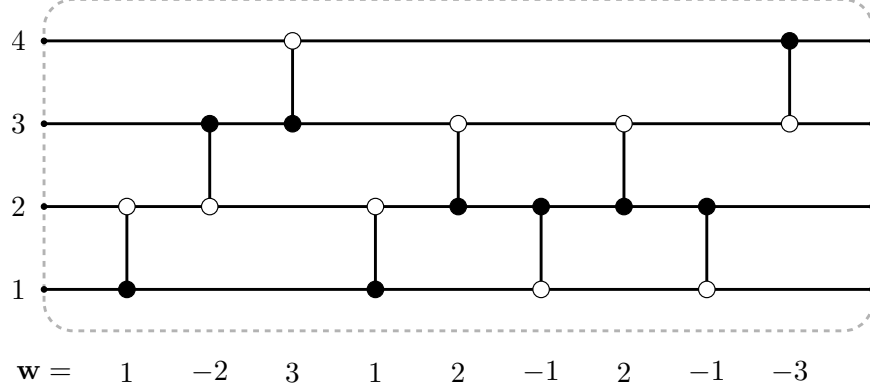
FIGURE 26.   The plabic fence $G(\mathbf{w})$ for a double braid word $\mathbf{w}$.

(B4) $(-i, \dots) \leftrightarrow (i, \dots)$ for $i \in \pm I$;
(B5) $(\dots, -i) \leftrightarrow (\dots, i)$ for $i \in \pm I$.

It is clear that if $\mathbf{w}, \mathbf{w}' \in (\pm I)^m$ are double braid move equivalent then the plabic graphs $G(\mathbf{w}), G(\mathbf{w}')$ are move equivalent.

Proposition 7.9. *Plabic fences are leaf recurrent. That is, for any double braid word $\mathbf{w} \in (\pm I)^m$, $G(\mathbf{w})$ is a leaf recurrent plabic graph.*

Proof. Proceed by induction on m. The base case $m = 0$ is clear.

Applying moves (B3)–(B4), we may assume that $\mathbf{w}$ has no negative indices. We say that a word $\mathbf{w} = (i_1, i_2, \dots, i_m) \in I^m$ is *reduced* if the associated permutation $\pi(\mathbf{w}) := s_{i_1} s_{i_2} \cdots s_{i_m}$ has precisely m inversions. If $\mathbf{w}$ is not reduced then we may apply moves (B1)–(B2) to transform $\mathbf{w}$ into a word of the form $(\mathbf{w}_1, i, i, \mathbf{w}_2)$ for some $i \in I$ and some words $\mathbf{w}_1 \in I^{m_1}$, $\mathbf{w}_2 \in I^{m_2}$. Let $-\operatorname{rev}(\mathbf{w}_1) \in (-I)^{m_1}$ denote the word obtained from $\mathbf{w}_1$ by negating all indices and reversing their order. One can transform $\mathbf{w}_1$ into $-\operatorname{rev}(\mathbf{w}_1)$ by applying moves (B3)–(B4). Thus, applying moves (B3)–(B4), we transform

$$(\mathbf{w}_1, i, i, \mathbf{w}_2) \to (-\operatorname{rev}(\mathbf{w}_1), i, i, \mathbf{w}_2) \to (i, i, \mathbf{w}_2, -\operatorname{rev}(\mathbf{w}_1)) \to (i, i, \mathbf{w}_2, \mathbf{w}_1).$$

The double bridge in $G(i, i, \mathbf{w}_2, \mathbf{w}_1)$ corresponding to $(i, i, \dots)$ gives rise to a boundary leaf face. Applying the induction hypothesis to the words $\mathbf{w}' := (i, \mathbf{w}_2, \mathbf{w}_1)$ and $\mathbf{w}'' := (\mathbf{w}_2, \mathbf{w}_1)$, we see that the plabic graphs $G(\mathbf{w}')$ and $G(\mathbf{w}'')$ are leaf recurrent. Thus, by Definition 7.3, $G(\mathbf{w})$ is also a leaf recurrent plabic graph.

Finally, suppose that the word $\mathbf{w} = (i_1, i_2, \dots, i_m) \in I^m$ is reduced. Then $G(\mathbf{w})$ is a reduced plabic graph and therefore we are done by Theorem 7.5. Alternatively, applying moves (B3)–(B4), we may transform $\mathbf{w}$ as follows:

$$(i_1, i_2, \dots, i_m) \to (-i_1, i_2, \dots, i_m) \to (i_2, \dots, i_m, -i_1) \to (i_2, \dots, i_m, i_1).$$

We refer to this transformation as a *conjugation move*. Applying conjugation and braid moves repeatedly, we either arrive at a non-reduced word and proceed by induction, or we find that $\pi(\mathbf{w}) \in S_N$ is a minimal length representative in its conjugacy class; see [GP93, Theorem 1.1]. Recall that conjugacy classes in the symmetric group S_N correspond to cycle types, and $\pi(\mathbf{w})$ has minimal length if and only if it is a product of cycles of the form $(a, a+1, \dots, b)$ on disjoint intervals $[a, b] \subset [N]$. The resulting plabic fence $G(\mathbf{w})$ has no interior faces and therefore is leaf recurrent.   □

8. Invariants of quivers and links

In this section, we investigate the relation between some other invariants of the quiver Q_G and invariants of the link L_G^{plab}.

8.1. Corank.
Recall that we set $\mathrm{corank}(Q) := \mathrm{corank}(B(Q)) = n - \mathrm{rank}(B(Q))$ for a quiver Q with n vertices.

Proposition 8.1. *Let G be a plabic graph. Then*
$$\mathrm{c}(G) + \mathrm{corank}(Q_G) = \mathrm{c}(L_G^{\mathrm{plab}}).$$

Proof. We prove the result using the same induction as in the proof of Proposition 6.8. The result can be checked directly for the graphs in Figure 20. We now suppose that G has one of the following: (a) an interior leaf, or (b) a loop edge, or (c) two parallel edges between vertices of opposite color.

In case (a), removing the leaf vertex preserves $\mathrm{c}(G)$, $\mathrm{c}(L_G^{\mathrm{plab}})$, and $\mathrm{corank}(Q_G)$. In case (b), removing the loop edge reduces $\mathrm{c}(L_G^{\mathrm{plab}})$ by 1 and $\mathrm{corank}(Q_G)$ by 1. In case (c), we use the same notation as in the proof of Proposition 6.8; see Figure 24. Let G' be obtained from G by removing both edges e', e''. This operation preserves $\mathrm{c}(L_G^{\mathrm{plab}})$. If F', F'' are boundary faces, then $\mathrm{c}(G') = \mathrm{c}(G) + 1$ and $\mathrm{corank}(Q_G) = \mathrm{corank}(Q_G) - 1$. If one of the faces F', F'' is boundary and one is interior, then $\mathrm{c}(G') = \mathrm{c}(G)$ and $\mathrm{corank}(Q_{G'}) = \mathrm{corank}(Q_G)$, as shown in the proof of Proposition 6.8. If F', F'' are both interior, we may assume they are distinct. Thus, $\mathrm{c}(G') = \mathrm{c}(G)$ and as shown in the proof of Proposition 6.8, we have $\mathrm{corank}(Q_{G'}) = \mathrm{corank}(Q_G)$. Thus, $\mathrm{c}(Q_G) + \mathrm{corank}(Q_G) = \mathrm{c}(L_G^{\mathrm{plab}})$ follows from the same equation for G'. $\square$

Remark 8.2. For algebraic links, Proposition 8.1 should be compared to [FPST22, Proposition 4.7].

8.2. Catalan numbers.
Recall that for a quiver Q, we defined the Q-Catalan number in Definition 5.9.

Definition 8.3. Let L be a link and let $\tilde{P}(L; q) := (q - 1)^{\mathrm{c}(L)-1} P^{\mathrm{top}}(L; q)$. If $\tilde{P}(L; q)$ is a polynomial in q, define
$$\chi_L := \tilde{P}(L; 1).$$
We call χ_L the *Catalan number* of the link L, or simply the *L-Catalan number*.

See Table 2 for some examples.

Proposition 8.4. *Suppose that Conjecture 2.8 holds for a simple plabic graph G. Then* $\chi_{Q_G} = \chi_{L_G^{\mathrm{plab}}}$.

Proof. Let $\widetilde{Q}$ be a minimal extension of Q_G (cf. Corollary 6.9), and set $m = \mathrm{corank}(Q_G)$. Then
$$R(\widetilde{Q}; q) = (q-1)^m R(Q_G; q) = (q-1)^{m+\mathrm{c}(G)-1} P^{\mathrm{top}}(L_G^{\mathrm{plab}}; q) = (q-1)^{\mathrm{c}(L_G^{\mathrm{plab}})-1} P^{\mathrm{top}}(L_G^{\mathrm{plab}}; q)$$
by Conjecture 2.8 and Proposition 8.1. Thus, $\chi_Q = \chi_{L_G^{\mathrm{plab}}}$. $\square$

Problem 8.5.
- For which links is χ_L defined?
- For which links is χ_L nonnegative, or positive?

Example 8.6. Even when χ_L is defined, it may be negative. The smallest knot K for which this happens is listed as $12n_{199}$ in [LM22]. It has HOMFLY polynomial

$$P(K;q) = -\frac{1}{a^4} + \frac{z^6 + 6\,z^4 + 11\,z^2 + 6}{a^6} - \frac{z^4 + 4\,z^2 + 4}{a^8},$$

and therefore $\tilde{P}(K;q) = P^{\mathrm{top}}(K;q) = -q^2$, with $\chi_K = -1$.

8.3. **Cluster cohomology versus link homology.** Let Q be a locally acyclic and torsion-free quiver. Let $\widetilde{Q}$ be a minimal extension of Q and set $m = \mathrm{corank}(B(Q))$. Let $T = T(\widetilde{Q})$ be the cluster automorphism torus of $\widetilde{Q}$ defined in [LS22, Section 5]. The torus T acts on $\mathcal{A}(\widetilde{Q})$ sending every cluster variable to a nonzero multiple of itself, and the character lattice of T is naturally identified with $\mathbb{Z}^{n+m}/\widetilde{B}(\widetilde{Q})\mathbb{Z}^n$.

We may associate to Q the cohomology and the compactly-supported T-equivariant cohomology of the cluster variety $\mathcal{X}(\widetilde{Q})$. Both cohomologies are equipped with mixed Hodge structures

$$H^*(\mathcal{X}(\widetilde{Q})) = \bigoplus_{k,p,q} H^{k,(p,q)}(\mathcal{X}(\widetilde{Q});\mathbb{C}) \qquad \text{and} \qquad H^*_{T,c}(\mathcal{X}(\widetilde{Q})) = \bigoplus_{k,p,q} H^{k,(p,q)}_{T,c}(\mathcal{X}(\widetilde{Q});\mathbb{C}).$$

Proposition 8.7. *The cohomology* $H^*(Q) := H^*(\mathcal{X}(\widetilde{Q}))$ *is of* mixed Tate type, *that is,*

$$H^*(\mathcal{X}(\widetilde{Q})) = \bigoplus_{k,p} H^{k,(p,p)}(\mathcal{X}(\widetilde{Q});\mathbb{C}).$$

Moreover, it does not depend on the choice of $\widetilde{Q}$.

Proof. The first statement is part of [LS22, Theorem 8.3]. Let $\widetilde{Q}$ and $\widetilde{Q}'$ be two really full rank ice quivers with mutable part Q and the same number m of frozen variables. In [LS22, Proposition 5.11], it is shown that we have an isomorphism of mixed Hodge structures $H^*(\mathcal{X}(\widetilde{Q})) = H^*(\mathcal{X}(\widetilde{Q}'))$. $\square$

The results of [LS22] are only established in the case of ordinary cohomology. In the following, we assume that the results there extend to equivariant cohomology. That is, we have

$$H^*_{T,c}(Q) := H^*_{T,c}(\mathcal{X}(\widetilde{Q})) = \bigoplus_{k,p} H^{k,(p,p)}_{T,c}(\mathcal{X}(\widetilde{Q});\mathbb{C})$$

and it does not depend on the choice of $\widetilde{Q}$. We expect to return to equivariant cohomology of cluster varieties in future work.

Let L be an oriented link. Let $H\!H\!H(L)$ denote the Khovanov–Rozansky triply-graded homology [KR08a, KR08b, Kho07] of L, and $H\!H\!H^0(L)$ the Hochschild degree 0 part of $H\!H\!H(L)$. Similarly, let $H\!H\!H_\mathbb{C}$ denoted the variant of Khovanov–Rozansky homology defined in [GL20, Section 3], and let $H\!H\!H^0_\mathbb{C}$ denote the Hochschild degree 0 part. We assume these homology groups have been normalized so they become link invariants; cf. [GL20, Equations (3.11) and (3.15)].

Conjecture 8.8. *Let* G *be a connected simple plabic graph. Then we have bigraded isomorphisms*

$$H^*(Q_G) \cong H\!H\!H^0_\mathbb{C}(L_G^{\mathrm{plab}}) \qquad \text{and} \qquad H^*_{T,c}(Q_G) \cong H\!H\!H^0(L_G^{\mathrm{plab}}).$$

We refer the reader to [GL20] for the precise correspondence between the bigradings. Here are some comments on Conjecture 8.8:

(1) The torus T has dimension $m = \operatorname{corank}(B(Q))$, which by Proposition 8.1 equals to $\mathrm{c}(L_G^{\mathrm{plab}}) - 1$, where $\mathrm{c}(L_G^{\mathrm{plab}})$ is the number of connected components of L_G^{plab}.

(2) The Khovanov–Rozansky homology $H\!H\!H(L_G^{\mathrm{plab}})$ has an action of a polynomial ring with $\mathrm{c}(L_G^{\mathrm{plab}}) - 1$ generators. This action should correspond to the action of $H_T^*(\mathrm{pt})$ on $H_{T,c}^*(Q_G)$.

(3) The Euler characteristic of $H\!H\!H(L)$ recovers the HOMFLY polynomial $P(L)$; see [GL20, (3.13)]. Thus, taking the Euler characteristic of Conjecture 8.8 produces Conjecture 2.8.

(4) When $m = \operatorname{corank}(B(G)) = 0$, the torus T is the trivial group. In this case $H_{T,c}^*(\mathcal{X}(\widetilde{Q})) = H_c^*(\mathcal{X}(\widetilde{Q}))$, so $H^*(Q_G)$ and $H_{T,c}^*(Q_G)$ are related by Poincare duality. Thus, Conjecture 8.8 predicts that the ordinary cohomology $H^*(Q_G)$ is identified with the degree 0 part $H\!H\!H^0(L_G^{\mathrm{plab}})$ of the Khovanov–Rozansky homology.

(5) When G is a reduced plabic graph with N boundary vertices, Conjecture 8.8 is proven in [GL20]. Let $\widetilde{Q}_G$ be the ice quiver associated to G, with frozen vertices corresponding all but one of the boundary faces; see [GL19]. Then $\widetilde{Q}_G$ is a really full rank quiver, and $\mathcal{X}(\widetilde{Q}_G)$ is isomorphic to an open positroid variety Π_f° sitting inside a Grassmannian $\mathrm{Gr}(k, n)$.

In [GL20], we considered the action of the $(N-1)$-dimensional torus $T' \subset \mathrm{PGL}_N$ acting on Π_f°. When G is connected, the positroid $\mathcal{M}$ associated to Π_f° is connected as a matroid and the action of T' on Π_f° is faithful, for example by [AHLS21, Lemma 3.1]. It is straightforward to verify that T' acts on Π_f° by cluster automorphisms. In this case, $\widetilde{Q}_G$ has $(N-1)$ frozen vertices and $T(\widetilde{Q}_G)$ is also $(N-1)$-dimensional. It follows that we have an inclusion $T' \hookrightarrow T(\widetilde{Q}_G)$ where $T(\widetilde{Q}_G)/T'$ is a finite group. This finite group can be shown to be trivial, for example with the same argument as the proof of [AHLS21, Lemma 4.6]. If G is not connected, the torus T' does not act faithfully on Π_f°. Instead, we have a decomposition $T' \cong T'' \times T(\widetilde{Q}_G)$ where T'' acts trivially.

Finally, we remark that the number of frozen vertices in $\widetilde{Q}_G$ may not equal to $\operatorname{corank}(Q_G)$; nevertheless, the computation of $H_{T,c}^*(\mathcal{X}(\widetilde{Q}_G))$ and $H_{T,c}^*(Q_G)$ are essentially equivalent.

(6) When G is a plabic fence, the cluster variety is, up to a torus factor, a *double Bott–Samelson variety* in the sense of Shen–Weng [SW21]. By combining the cluster structure results of [SW21] with results on the cohomology of braid varieties [Tri21] (see [CGGS21, Remark 4.12]), one can deduce a version of Conjecture 8.8 for plabic fences. The point count of these cluster varieties is also discussed in [SW21, Corollary 6.7].

9. Conjectures and examples

9.1. **Example: a simple plabic graph that is not leaf recurrent.** Consider the plabic graph G in Figure 8(a). The associated quiver Q_G is mutation equivalent to an acyclic triangle quiver, with a single edge between each vertex of the triangle. In particular, Q_G is locally acyclic. However, it is easy to check that G is not a leaf recurrent plabic graph. Nevertheless, Conjecture 2.8 still holds for G. By Proposition 5.8, we have

$$R(Q_G; q) = (q-1)^3 + 3q(q-1) = q^3 - 1.$$

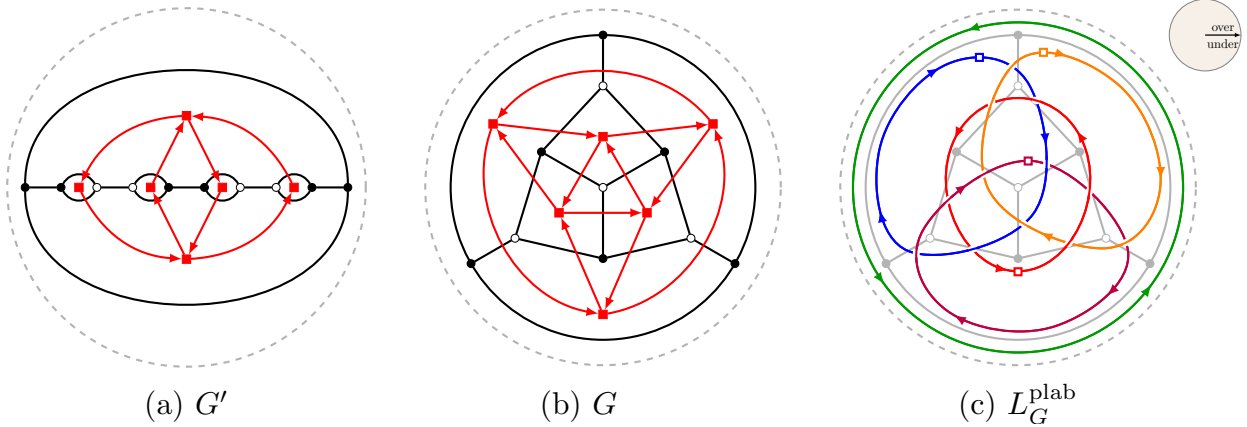(a) G' (b) G (c) L_G^{plab}

FIGURE 27. Two connected simple plabic graphs G, G' which are move equivalent. The associated quivers $Q_G, Q_{G'}$ are not locally acyclic.

On the other hand, the plabic graph link L_G^{plab} is listed as `L9n19` in [KAT1]. Its HOMFLY polynomial is given by

$$P(L_G^{\text{plab}}; a, z) = \frac{z^3 + 3z}{a^3} + \frac{z + z^{-1}}{a^7} - \frac{z^{-1}}{a^9}.$$

This agrees with Conjectures 2.8 and 6.3.

9.2. **Example: a simple plabic graph quiver that is not locally acyclic.** Consider the plabic graph G and the associated quiver Q_G in Figure 27(b). This quiver comes from a cluster algebra associated with a 4-punctured sphere; see [Mul13, Section 11.5].

Muller defines a cluster variety to be *locally acyclic* if it can be covered by cluster localizations that are acyclic.

Proposition 9.1 ([Mul13, Section 11.5])**.** *The quiver Q_G is not locally acyclic. The associated cluster algebra $\mathcal{A}(Q_G)$ is not locally acyclic.*

Proof. If Q_G is locally acyclic then $\mathcal{A}(Q_G)$ would be locally acyclic, so it is enough to establish the second statement. The proof in [Mul13] that $\mathcal{A}(Q_G)$ is not locally acyclic has the following gap: in [Mul13, Theorem 8.3], it is assumed that it is enough to check the cluster exchange relations to produce a point of a cluster variety. However, the ideal of relations between cluster variables is in general larger than the ideal generated by the exchange relations. G. Muller has supplied us with the following alternative argument.

The cluster algebra $\mathcal{A}(Q_G)$ includes into the tagged skein algebra $S_{q=1}$ at $q = 1$ of the 4-punctured sphere. This is the algebra generated by immersed curves in the surface with taggings at each puncture, modulo certain relations [Mul16]. The two algebras $\mathcal{A}(Q_G)$ and $S_{q=1}$ may or may not be equal. One can define a point p_0 in $\text{Spec}(S_{q=1})$ by giving every arc the value 0, and giving every loop the value $2(-1)^i$, where i is the number of punctures in the interior of the loop. The point p_0 defines a point in $\text{Spec}(\mathcal{A}(Q_G))$, and since every arc takes value 0 on p_0, so does every cluster variable. Since every cluster variable vanishes on p_0, it cannot be contained in any proper cluster localization (see [Mul13, Definition 3.3]). Therefore, p_0 cannot be contained in any locally acyclic cover of $\text{Spec}(\mathcal{A}(Q_G))$. $\qquad\square$

We do not know the point count function $R(Q; q)$ of this quiver, or even whether it is a polynomial. On the other hand, the HOMFLY polynomial of the link L_G^{plab} (see Figure 27(c))
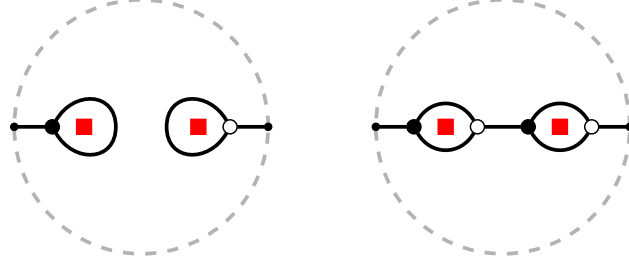
FIGURE 28. Two plabic graphs G (left) and G' (right) with the same quiver $Q_G = Q_{G'}$.

is given by

$$P(L_G^{\text{plab}}; a, z) = \frac{z^6 + 6z^4 + 11z^2 + 12 + 6z^{-2} + z^{-4}}{a^6} - \frac{2z^4 + 14z^2 + 27 + 19z^{-2} + 4z^{-4}}{a^8}$$
$$+ \frac{3(z^2 + 6 + 7z^{-2} + 2z^{-4})}{a^{10}} - \frac{3 + 9z^{-2} + 4z^{-4}}{a^{12}} + \frac{z^{-2} + z^{-4}}{a^{14}}.$$

Thus, according to Conjecture 2.8, the prediction for the point count $R(Q; q)$ is

$$\frac{q^{10} - 4q^9 + 8q^8 - 6q^7 - 3q^6 + 9q^5 - 3q^4 - 6q^3 + 8q^2 - 4q + 1}{(q-1)^4}.$$

9.3. **Example: conjectures fail when the plabic graph is not simple.** The plabic graph G in Figure 8(d) is not simple as the directed graph Q_G has a loop arrow. If we remove this loop, we obtain the quiver $Q := Q_G^- = A_1 \sqcup A_1$ consisting of two isolated vertices. The quiver point count is

$$(9.1) \qquad\qquad R(Q; q) = \left(\frac{q^2 - q + 1}{q - 1} \right)^2.$$

On the other hand, the link L_G^{plab} is listed as `L10n94` in [KAT1]. Its HOMFLY polynomial is

$$P(L_G^{\text{plab}}; a, z) = \frac{z^2 + 2}{a^2} - \frac{z^2 + 2z^{-2} + 3}{a^6} + \frac{z^{-2}}{a^4} + \frac{1 + z^{-2}}{a^8}.$$

Thus, Conjecture 2.8 predicts that the point count $R(Q; q)$ should be equal to $q^2 + 1$, which does not match (9.1).

The plabic graph G in Figure 8(b) is not simple as the directed graph Q_G has a directed 2-cycle. If we cancel out the arrows in this 2-cycle, we obtain a quiver $Q := Q_G^-$ that is a directed 4-cycle, which is mutation equivalent to the quiver of type D_4. Using Proposition 5.8, we obtain that the quiver point count is $R(D_4; q) = (q^6 - 2q^5 + 2q^4 - q^3 + 2q^2 - 2q + 1)/(q-1)^2$; see Table 1. On the other hand, the HOMFLY polynomial of L_G^{plab} is

$$P(L_G^{\text{plab}}; a, z) = \frac{z^4 + 4z^2 + 2}{a^4} - \frac{z^2 + 3 + 2z^{-2}}{a^{10}} + \frac{z^{-2}}{a^8} + \frac{1 + z^{-2}}{a^{12}}.$$

Thus, Conjecture 2.8 predicts that the point count $R(Q; q)$ should be given by $q^4 + 1$, which does not agree with $R(D_4; q)$.

9.4. **Connected sum and disjoint union.** Consider the graphs G and G' in Figure 28. The quiver $Q = Q_G = Q_{G'}$ satisfies

$$R(Q; q) = \left(\frac{q^2 - q + 1}{q - 1} \right)^2.$$

However, the links L_G^{plab} and $L_{G'}^{\text{plab}}$ are not isotopic: L_G^{plab} is a disjoint union of two Hopf links while $L_{G'}^{\text{plab}}$ is a connected sum of two Hopf links. The HOMFLY polynomials are given by

$$P(L_G^{\text{plab}}; a, z) = \left(\frac{a - a^{-1}}{z} \right) \left(\frac{z + z^{-1}}{a} - \frac{z^{-1}}{a^3} \right)^2;$$

$$P(L_{G'}^{\text{plab}}; a, z) = \left(\frac{z + z^{-1}}{a} - \frac{z^{-1}}{a^3} \right)^2.$$

We see that the HOMFLY polynomials of these two links are different, however, their top a-degree terms satisfy

$$(q - 1)P^{\text{top}}(L_G^{\text{plab}}; q) = P^{\text{top}}(L_{G'}^{\text{plab}}; q) = R(Q; q),$$

in agreement with Conjecture 2.8. We conjecture that when one restricts to the class of *connected* plabic graphs, the full HOMFLY polynomial becomes an invariant of the quiver.

Conjecture 9.2. *Let G, G' be two connected simple plabic graphs. Assume that the quivers Q_G and $Q_{G'}$ are mutation equivalent. Then*

$$P(L_G^{\text{plab}}; a, z) = P(L_{G'}^{\text{plab}}; a, z).$$

Remark 9.3. A stronger cohomological version of Conjecture 9.2 is that $\mathit{HHH}_{\mathbb{C}}(L_G^{\text{plab}}) \cong \mathit{HHH}_{\mathbb{C}}(L_{G'}^{\text{plab}})$ and $\mathit{HHH}(L_G^{\text{plab}}) \cong \mathit{HHH}(L_{G'}^{\text{plab}})$; see Section 8.3.

Remark 9.4. Let G be a reduced plabic graph with strand permutation $\pi = \pi_G$. The top a-degree coefficient $P^{\text{top}}(L_G^{\text{plab}}; q)$ of $P(L_G^{\text{plab}}; a, z)$ can be extracted from the open positroid variety Π_π° by computing the point count. However, observe that the first two rows in Figure 9 correspond to isomorphic open positroid varieties. Thus, neither the link L_G^{plab} nor the full HOMFLY polynomial $P(L_G^{\text{plab}}; a, z)$ are determined by Π_π°. Conjecture 9.2 implies that when G is connected, $P(L_G^{\text{plab}}; a, z)$ is fully determined by Π_π°. It would be interesting to find a geometric interpretation of the lower a-degree coefficients in this case.

Remark 9.5. According to M. Shapiro's conjecture [FPST22, Conjecture 6.17], if the quivers Q_G and $Q_{G'}$ are mutation equivalent then the graphs G and G' are *move-and-switch equivalent*. When two plabic graphs G, G' differ by a switch (see [FPST22, Figure 25]), the corresponding links $L_G^{\text{plab}}, L_{G'}^{\text{plab}}$ need not be isotopic. Nevertheless, by [FPST22, Proposition 6.16], Conjecture 9.2 implies $P(L_G^{\text{plab}}; a, z) = P(L_{G'}^{\text{plab}}; a, z)$. The switch operation can be defined more generally for oriented links, and we expect that this operation still preserves the HOMFLY polynomial.

Conjecture 9.6 (Switch preserves HOMFLY). *Suppose that the planar diagram of a link L intersects the vertical line $x = 0$ at four points $(0, -b)$, $(0, -a)$, $(0, a)$, $(0, b)$ for $0 < a < b$. Suppose that L is directed to the right at $(0, \pm b)$ and to the left at $(0, \pm a)$. The* switch *of L is a new link L' obtained by taking the $x > 0$ part of L and reflecting it along the x axis, flipping all crossings. Then*
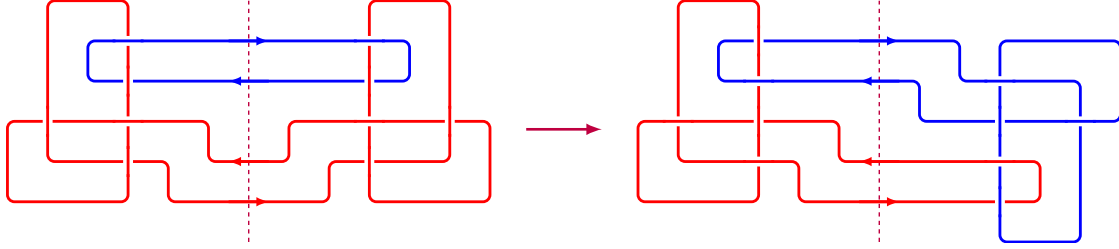
$$P(L; a, z) = P(L'; a, z).$$

FIGURE 29. The switch operation for links; see Conjecture 9.6.

K	χ_K	$P^{\mathrm{top}}(K;q)$	K	χ_K	$P^{\mathrm{top}}(K;q)$
3_1	2	$q^2 + 1$	9_5	0	$q^2 - 2q + 1$
5_1	3	$q^4 + q^2 + 1$	9_6	3	$q^6 - q^5 + 2q^4 - q^3 + 2q^2 - q + 1$
5_2	1	$q^2 - q + 1$	9_7	2	$q^4 - q^3 + 2q^2 - q + 1$
7_1	4	$q^6 + q^4 + q^2 + 1$	9_9	2	$q^6 - q^5 + 2q^4 - 2q^3 + 2q^2 - q + 1$
7_2	1	$q^2 - q + 1$	9_{10}	0	$q^4 - 2q^3 + 2q^2 - 2q + 1$
7_3	1	$q^4 - q^3 + q^2 - q + 1$	9_{13}	0	$q^4 - 2q^3 + 2q^2 - 2q + 1$
7_4	0	$q^2 - 2q + 1$	9_{16}	4	$q^6 - q^5 + 3q^4 - 2q^3 + 3q^2 - q + 1$
7_5	2	$q^4 - q^3 + 2q^2 - q + 1$	9_{18}	1	$q^4 - 2q^3 + 3q^2 - 2q + 1$
8_{15}	1	$q^4 - 2q^3 + 3q^2 - 2q + 1$	9_{23}	1	$q^4 - 2q^3 + 3q^2 - 2q + 1$
8_{19}	5	$q^6 + q^4 + q^3 + q^2 + 1$	9_{35}	0	$q^2 - 2q + 1$
8_{21}	3	$2q^2 - q + 2$	9_{38}	0	$q^4 - 3q^3 + 4q^2 - 3q + 1$
9_1	5	$q^8 + q^6 + q^4 + q^2 + 1$	9_{45}	2	$2q^2 - 2q + 2$
9_2	1	$q^2 - q + 1$	9_{46}	2	2
9_3	1	$q^6 - q^5 + q^4 - q^3 + q^2 - q + 1$	9_{49}	0	$q^4 - 2q^3 + 2q^2 - 2q + 1$
9_4	1	$q^4 - q^3 + q^2 - q + 1$			

TABLE 2. "Point counts" of small knots and the associated Catalan numbers.

See Figure 29 for an example of a switch.

9.5. **Small knots.** It is natural to ask which knots and links can potentially be associated to a quiver. Assuming Conjecture 2.8, a necessary condition for a link L to come from a locally acyclic quiver would be that up to a power of $(q-1)$, $P^{\mathrm{top}}(L;q)$ is a polynomial in q.

First, let K be the trefoil knot (Figure 9), with $P(K;q) = \frac{z^2+2}{a^2} - \frac{1}{a^4}$. Let K^* be the mirror image of K. Taking the mirror image results in replacing a with $-a^{-1}$; cf. (2.3). Thus, $P(K^*;q) = -a^4 + (z^2+2)a^2$ and $P^{\mathrm{top}}(K^*;q) = -q^{-2}$, which is not a polynomial. Next, let E be the figure-eight knot. It coincides with its mirror image: $E \cong E^*$. We have $P(E;q) = a^2 - (z^2+1) + \frac{1}{a^2}$ and $P^{\mathrm{top}}(E;q) = -q^{-1}$, which is again not a polynomial. We therefore do not expect K^* and E to be associated to locally acyclic quivers. (By [GL20, Theorem 1.11], it follows that neither K^* nor E is a Richardson knot.)

In Table 2, we give a list of all knots K with up to 9 crossings such that $P^{\mathrm{top}}(K;q)$ is a polynomial in q. The knot numbering is taken from [Rol90, KAT2], and the knots are considered up to taking the mirror image. We see that for $K = 8_{21}$, the leading coefficient of $P^{\mathrm{top}}(K;q)$ is 2, which violates Conjecture 6.3; thus, we do not expect 8_{21} to be associated to a quiver.
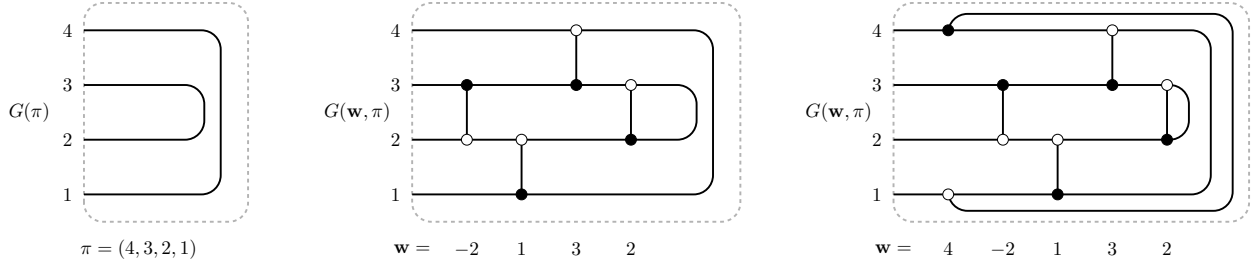
FIGURE 30.   A reduced plabic graph $G(\pi)$ and two affine plabic fences.

9.6. **Affine plabic fences.** While reduced plabic graphs were classified by Postnikov [Pos06], the problem of classifying simple plabic graphs appears much harder. We consider an affine version of plabic fences, which contains a large subclass of simple plabic graphs that can be parametrized; see Proposition 9.7.

Fix $N \geq 2$. Let $\tilde{I} := I \sqcup \{N\} = \{1, 2, \ldots, N-1, N\}$. A *double affine braid word* is a word $\mathbf{w} = (i_1, i_2, \ldots, i_m)$ in the alphabet

$$\pm \tilde{I} := \{-1, -2, \ldots, -N\} \sqcup \{1, 2, \ldots, N\}.$$

Recall from [Pos06] that for any (k, N)-bounded affine permutation $f \in \mathrm{Bound}(k, N)$, we have a reduced plabic graph $G(f)$, satisfying the conditions of Section 2.2. For each fixed point $i \in [N]$ of $\pi := \bar{f} \in S_N$, the boundary vertex i of $G(f)$ is adjacent to an interior leaf, called a *lollipop*. This lollipop is white if $f(i) = i + N$ and black if $f(i) = i$. In particular, if π has no fixed points then $G(f)$ has no interior leaves. Recall from Section 3.1 that in this case, f can be recovered from π, and we denote $G(\pi) := G(f)$.

Given a double affine braid word $\mathbf{w} = (i_1, i_2, \ldots, i_m)$, and $f \in \mathrm{Bound}(k, N)$, we define the *affine plabic fence* $G(\mathbf{w}, f)$ as follows. Begin with the plabic graph $G(f)$. For each $j = m, m-1, \ldots, 1$, let $h := |i_j|$ and consider the two boundary vertices h and $h+1$, considered modulo N. If $i_j > 0$, add a black at h, white at $h+1$ bridge between these two boundary vertices, and if $i_j < 0$, add a white at h, black at $h+1$ bridge between these two boundary vertices. When $\pi := \bar{f}$ has no fixed points, we denote $G(\mathbf{w}, \pi) := G(\mathbf{w}, f)$. See Figure 30 for an example.

Proposition 9.7. *For any* $\mathbf{w} \in (\pm\tilde{I})^m$ *and any permutation* $\pi \in S_N$ *without fixed points, the plabic graph* $G(\mathbf{w}, \pi)$ *is simple.*

Proof. It is clear from the construction that every time we add a bridge to an affine plabic fence, the faces F and F' on the two sides of the bridge are distinct. Thus, the quiver of $G(\mathbf{w}, \pi)$ cannot have 1-cycles. Let F, F' be two adjacent (interior or boundary) faces of $G(\mathbf{w}, \pi)$. If F and F' are both adjacent to the bridge e, then e must be the only edge separating F and F' since this is the case if e is the bridge added to $G(f)$.

In $G(f)$, any two faces have at most one edge in common. So if F and F' do not have a bridge edge in common in $G(\mathbf{w}, \pi)$, then their common boundary must belong to a single edge e' of $G(f)$. The edge e' is divided into a number of segments by the vertices of $G(\mathbf{w}, \pi)$ that lie on e'. By considering what happens when a single bridge is added, we see that two distinct such segments cannot belong to the boundary of the same two faces of $G(\mathbf{w}, \pi)$. It follows that the quiver of $G(\mathbf{w}, \pi)$ has no directed 2-cycles. $\qquad \square$

Not all simple affine plabic fences are leaf recurrent: for instance, the non-leaf recurrent example in Section 9.1 is move equivalent to the example in Figure 30(middle). It would be interesting to find a criterion for an affine plabic fence to be leaf recurrent.

We say that two indices $i, j \in \tilde{I}$ are *adjacent* if either $|i - j| = 1$ or $\{i, j\} = \{1, N\}$. Similarly, $i, j \in -\tilde{I}$ are *adjacent* if $|i|$ and $|j|$ are adjacent. Consider the following moves on double affine braid words:

(B̃1) $(\ldots, i, j, i, \ldots) \leftrightarrow (\ldots, j, i, j, \ldots)$ if $i, j \in \pm\tilde{I}$ have the same sign and are adjacent;
(B̃2) $(\ldots, i, j, \ldots) \leftrightarrow (\ldots, j, i, \ldots)$ if $i, j \in \pm\tilde{I}$ have the same sign and are non-adjacent;
(B̃3) $(\ldots, i, j, \ldots) \leftrightarrow (\ldots, j, i, \ldots)$ if $i, j \in \pm\tilde{I}$ have different signs;
(B̃4) $(-i, \ldots) \leftrightarrow (i, \ldots)$ for $i \in \pm\tilde{I}$;

If $\mathbf{w}, \mathbf{w}'$ are equivalent using (B̃1)–(B̃4), then $G(\mathbf{w}, f)$ and $G(\mathbf{w}', f)$ are move equivalent. If $\mathbf{w}, \mathbf{w}'$ are equivalent using (B̃1)–(B̃3), then $G(\mathbf{w}, f)$ and $G(\mathbf{w}', f)$ are move equivalent without using tail addition/removal, in which case we say that they are *restricted move equivalent*. In particular, the number of boundary vertices is fixed under restricted move equivalence. We now consider the question of the classification of affine plabic fences, up to restricted move equivalence. This is analogous to the classification of equivalence classes of reduced plabic graphs by Postnikov [Pos06].

Remark 9.8. For the rest of this subsection, we consider arbitrary bounded affine permutations $f \in \mathrm{Bound}(k, N)$, with no restrictions on fixed points. Consequently, we allow our plabic graphs to have interior vertices of degree 1, 2, or 3. Vertices of degree 2 can be freely placed on the edges and removed from them. If an interior leaf is connected to an interior vertex of the same color (as in the right two pictures in Figure 21), the edge connecting them may be contracted. Conversely, we can place a degree two vertex on any edge and attach a leaf of the same color to it. These extra moves are included in the notion of restricted move equivalence.

We say that $f \in \mathrm{Bound}(k, N)$ *has a left descent at* $i \in \mathbb{Z}$ if $i + 1 \leq f(i) < f(i+1) \leq i + n$. In this case, we let $s_i f : \mathbb{Z} \to \mathbb{Z}$ be the N-periodic bijection sending $i \mapsto f(i+1)$, $i+1 \mapsto f(i)$, and $j \mapsto f(j)$ for $j \not\equiv i, i + 1$ modulo N. Then we have $s_i f \in \mathrm{Bound}(k, N)$, and the plabic graph $G(f)$ is obtained from $G(s_i f)$ by adding a bridge that is white at i and black at $i + 1$. Similarly, $f \in \mathrm{Bound}(k, N)$ *has a right descent at* $i \in \mathbb{Z}$ if $i - n \leq f^{-1}(i) \leq f^{-1}(i + 1) \leq i$. In this case, we define $f s_i : \mathbb{Z} \to \mathbb{Z}$ to be the N-periodic bijection sending $f^{-1}(i) \mapsto i + 1$, $f^{-1}(i + 1) \mapsto i$, and $f^{-1}(j) \mapsto j$ for $j \not\equiv i, i + 1$ modulo N. We have $f s_i \in \mathrm{Bound}(k, N)$ and the plabic graph $G(f)$ is obtained from $G(f s_i)$ by adding a bridge that is black at i and white at $i + 1$. See [Lam16, Section 7.4]. Note that the graphs $G(s_i f)$ and $G(f s_i)$ may contain lollipops even when $G(f)$ does not.

We introduce two new moves for affine plabic fences:

(B̃5) $G(\mathbf{w}, f) \leftrightarrow G((\mathbf{w}, -i), s_i f)$ if f has a left descent at i;
(B̃6) $G(\mathbf{w}, f) \leftrightarrow G((\mathbf{w}, i), f s_i)$ if f has a right descent at i.

Note that these moves respect restricted move equivalence as they can be obtained from the extra plabic graph moves listed in Remark 9.8.

Conjecture 9.9. *Two affine plabic fences $G(\mathbf{w}, f)$ and $G(\mathbf{w}', f')$ are restricted move equivalent if and only if they can be related by moves (B̃1)–(B̃3) and (B̃5)–(B̃6).*

Remark 9.10. A strengthening of Conjecture 9.9 can be given when $f = f_{k,N}$ is the "top cell" bounded affine permutation (Section 3.1). Consider the affine braid group with generators $\beta_i^{\pm 1}$ for $i \in I$, lifting the Coxeter generators s_i, together with the shift braids that lift the affine permutations $i \mapsto i + k$. For a word $\mathbf{w} \in (\pm I)^m$, consider an affine braid $\mathbf{w}_1 f_{k,N} \mathbf{w}_2$, where $\mathbf{w}_1$ (resp., $\mathbf{w}_2$) is the positive braid lift of the subword of $\mathbf{w}$ consisting of the letters from $\tilde{I}$ (resp., positive braid lift of the reverse of the subword of $\mathbf{w}$ consisting of letters from $-\tilde{I}$). We conjecture that for $\mathbf{w}, \mathbf{w}' \in (\pm I)^m$, the affine plabic fences $G(\mathbf{w}, f_{k,N})$ and $G(\mathbf{w}', f_{k,N})$ are restricted move equivalent if and only if the affine braids $\mathbf{w}_1 f_{k,N} \mathbf{w}_2$ and $\mathbf{w}'_1 f_{k,N} \mathbf{w}'_2$ are braid equivalent, or equivalently, the affine braids $\mathbf{w}_1(\mathbf{w}_2 + k)$ and $\mathbf{w}'_1(\mathbf{w}'_2 + k)$ are braid equivalent, where $(\mathbf{w}_2 + k)$ is the positive braid word obtained by adding k (modulo N) to each letter in $\mathbf{w}_2$.

9.7. Trees and acyclic quivers.

Definition 9.11. A link L is called *acyclic* (resp. *tree-like*) if there is a simple plabic graph G such that $L = L_G^{\text{plab}}$, and Q_G is mutation acyclic (resp. mutation equivalent to a tree).

Problem 9.12.

- Which acyclic quivers Q can occur as Q_G for a simple plabic graph G?
- Can we characterize acyclic, or tree-like links?

It is clear that any tree T can occur as Q_G for some simple plabic graph G. In fact, Lam and Speyer (unpublished) have shown that one can choose such a plabic graph to be reduced.

We expect that acyclic links have particularly simple link invariants, including link homology groups. Proposition 5.8 gives a closed formula for the top a-degree part of the HOMFLY polynomial of an acyclic link. It would be interesting to obtain a closed formula for the entire HOMFLY polynomial.

In [LS21, Theorem 1.3], it is shown that the mixed Hodge numbers of an acyclic really full rank cluster variety satisfy a strong vanishing condition. It would be interesting to interpret this vanishing via the link homology groups of acyclic links.

References

[A'C99]   Norbert A'Campo. Real deformations and complex topology of plane curve singularities. *Ann. Fac. Sci. Toulouse Math. (6)*, 8(1):5–23, 1999.

[AHLS21]   Nima Arkani-Hamed, Thomas Lam, and Marcus Spradlin. Positive configuration space. *Comm. Math. Phys.*, 384(2):909–954, 2021.

[BHM⁺21] Jonah Blasiak, Mark Haiman, Jennifer Morse, Anna Pun, and George H. Seelinger. A Shuffle Theorem for Paths Under Any Line. `arXiv:2102.07931v1`, 2021.

[BMS21]   Véronique Bazier-Matte and Ralf Schiffler. Knot theory and cluster algebras. `arXiv:2110.14740v2`, 2021.

[BS12]   Igor Burban and Olivier Schiffmann. On the Hall algebra of an elliptic curve, I. *Duke Math. J.*, 161(7):1171–1231, 2012.

[CGG⁺22] Roger Casals, Eugene Gorsky, Mikhail Gorsky, Ian Le, Linhui Shen, and José Simental. Cluster structures on braid varieties. `arXiv:2207.11607v1`, 2022.

[CGGS21]   Roger Casals, Eugene Gorsky, Mikhail Gorsky, and José Simental. Positroid Links and Braid varieties. `arXiv:2105.13948v1`, 2021.

[CW22]   Roger Casals and Daping Weng. Microlocal theory of legendrian links and cluster algebras. `arXiv:2204.13244`, 2022.

[FPST22]   Sergey Fomin, Pavlo Pylyavskyy, Eugenii Shustin, and Dylan Thurston. Morsifications and mutations. *J. Lond. Math. Soc. (2)*, 105(4):2478–2554, 2022.

[FYH⁺85] P. Freyd, D. Yetter, J. Hoste, W. B. R. Lickorish, K. Millett, and A. Ocneanu. A new polynomial invariant of knots and links. *Bull. Amer. Math. Soc. (N.S.)*, 12(2):239–246, 1985.

[FZ02] Sergey Fomin and Andrei Zelevinsky. Cluster algebras. I. Foundations. *J. Amer. Math. Soc.*, 15(2):497–529 (electronic), 2002.

[GL19] Pavel Galashin and Thomas Lam. Positroid varieties and cluster algebras. *Ann. Sci. Éc. Norm. Supér.,* to appear. `arXiv:1906.03501v2`, 2019.

[GL20] Pavel Galashin and Thomas Lam. Positroids, knots, and q,t-Catalan numbers. `arXiv:2012.09745v2`, 2020.

[GL21] Pavel Galashin and Thomas Lam. Positroid Catalan numbers. `arXiv:2104.05701v1`, 2021.

[GLSBSa] Pavel Galashin, Thomas Lam, Melissa Sherman-Bennett, and David Speyer. Braid variety cluster structures, I: 3D plabic graphs. *In preparation.*

[GLSBSb] Pavel Galashin, Thomas Lam, Melissa Sherman-Bennett, and David Speyer. Braid variety cluster structures, II: general type. *In preparation.*

[GN15] Eugene Gorsky and Andrei Neguţ. Refined knot invariants and Hilbert schemes. *J. Math. Pures Appl. (9)*, 104(3):403–435, 2015.

[GNR21] Eugene Gorsky, Andrei Neguţ, and Jacob Rasmussen. Flag Hilbert schemes, colored projectors and Khovanov-Rozansky homology. *Adv. Math.*, 378:107542, 115, 2021.

[GP93] Meinolf Geck and Götz Pfeiffer. On the irreducible characters of Hecke algebras. *Adv. Math.*, 102(1):79–94, 1993.

[HI15] Kazuhiro Hikami and Rei Inoue. Braids, complex volume and cluster algebras. *Algebr. Geom. Topol.*, 15(4):2175–2194, 2015.

[Hir02] Mikami Hirasawa. Visualization of A'Campo's fibered links and unknotting operation. In *Proceedings of the First Joint Japan-Mexico Meeting in Topology (Morelia, 1999)*, volume 121, pages 287–304, 2002.

[KAT1] The Knot Atlas: The Thistlethwaite Link Table, `http://katlas.org/wiki/The_Thistlethwaite_Link_Table`.

[KAT2] The Knot Atlas: The Rolfsen Knot Table, `http://katlas.org/wiki/The_Rolfsen_Knot_Table`.

[Kho07] Mikhail Khovanov. Triply-graded link homology and Hochschild homology of Soergel bimodules. *Internat. J. Math.*, 18(8):869–885, 2007.

[KLS13] Allen Knutson, Thomas Lam, and David E. Speyer. Positroid varieties: juggling and geometry. *Compos. Math.*, 149(10):1710–1752, 2013.

[KR08a] Mikhail Khovanov and Lev Rozansky. Matrix factorizations and link homology. *Fund. Math.*, 199(1):1–91, 2008.

[KR08b] Mikhail Khovanov and Lev Rozansky. Matrix factorizations and link homology. II. *Geom. Topol.*, 12(3):1387–1425, 2008.

[Lam16] Thomas Lam. Totally nonnegative Grassmannian and Grassmann polytopes. In *Current developments in mathematics 2014*, pages 51–152. Int. Press, Somerville, MA, 2016.

[Lec16] B. Leclerc. Cluster structures on strata of flag varieties. *Adv. Math.*, 300:190–228, 2016.

[Lic97] W. B. Raymond Lickorish. *An introduction to knot theory*, volume 175 of *Graduate Texts in Mathematics*. Springer-Verlag, New York, 1997.

[LM22] Charles Livingston and Allison H. Moore. Knotinfo: Table of knot invariants. URL: `knotinfo.math.indiana.edu`, July 2022.

[LS19] Kyungyong Lee and Ralf Schiffler. Cluster algebras and Jones polynomials. *Selecta Math. (N.S.)*, 25(4):Paper No. 58, 41, 2019.

[LS21] Thomas Lam and David E. Speyer. Cohomology of cluster varieties. II. Acyclic case. `arXiv:2111.12759v1`, 2021.

[LS22] Thomas Lam and David E. Speyer. Cohomology of cluster varieties I: Locally acyclic case. *Algebra Number Theory*, 16(1):179–230, 2022.

[Mel19] Anton Mellit. Cell decompositions of character varieties. `arXiv:1905.10685v1`, 2019.

[MS16] Greg Muller and David E. Speyer. Cluster algebras of Grassmannians are locally acyclic. *Proc. Amer. Math. Soc.*, 144(8):3267–3281, 2016.

[Mul13] Greg Muller. Locally acyclic cluster algebras. *Adv. Math.*, 233:207–247, 2013.

[Mul16] Greg Muller. Skein and cluster algebras of marked surfaces. *Quantum Topol.*, 7(3):435–503, 2016.

[OR17]   Alexei Oblomkov and Lev Rozansky. HOMFLYPT homology of Coxeter links. `arXiv:1706.00124v2`, 2017.

[OSS15]   Peter S. Ozsváth, András I. Stipsicz, and Zoltán Szabó. *Grid homology for knots and links*, volume 208 of *Mathematical Surveys and Monographs*. American Mathematical Society, Providence, RI, 2015.

[Pos06]   Alexander Postnikov. Total positivity, Grassmannians, and networks. Preprint, `http://math.mit.edu/~apost/papers/tpgrass.pdf`, 2006.

[PT87]   Józef H. Przytycki and Pawel Traczyk. Conway algebras and skein equivalence of links. *Proc. Amer. Math. Soc.*, 100(4):744–748, 1987.

[Rol90]   Dale Rolfsen. *Knots and links*, volume 7 of *Mathematics Lecture Series*. Publish or Perish, Inc., Houston, TX, 1990. Corrected reprint of the 1976 original.

[Sco06]   J. S. Scott. Grassmannians and cluster algebras. *Proc. London Math. Soc. (3)*, 92(2):345–380, 2006.

[SSBW19] K. Serhiyenko, M. Sherman-Bennett, and L. Williams. Cluster structures in Schubert varieties in the Grassmannian. *Proc. Lond. Math. Soc. (3)*, 119(6):1694–1744, 2019.

[STWZ19] Vivek Shende, David Treumann, Harold Williams, and Eric Zaslow. Cluster varieties from Legendrian knots. *Duke Math. J.*, 168(15):2801–2871, 2019.

[STZ17]   Vivek Shende, David Treumann, and Eric Zaslow. Legendrian knots and constructible sheaves. *Invent. Math.*, 207(3):1031–1133, 2017.

[SV13]   Olivier Schiffmann and Eric Vasserot. The elliptic Hall algebra and the K-theory of the Hilbert scheme of $\mathbb{A}^2$. *Duke Math. J.*, 162(2):279–366, 2013.

[SW21]   Linhui Shen and Daping Weng. Cluster structures on double Bott-Samelson cells. *Forum Math. Sigma*, 9:Paper No. e66, 89, 2021.

[Tri21]   Minh-Tâm Quang Trinh. From the Hecke Category to the Unipotent Locus. `arXiv:2106.07444v2`, 2021.

[Tur88]   V. G. Turaev. The Conway and Kauffman modules of a solid torus. *Zap. Nauchn. Sem. Leningrad. Otdel. Mat. Inst. Steklov. (LOMI)*, 167(Issled. Topol. 6):79–89, 190, 1988.

Department of Mathematics, University of California, Los Angeles, 520 Portola Plaza, Los Angeles, CA 90025, USA

  Email address: `galashin@math.ucla.edu`

Department of Mathematics, University of Michigan, 2074 East Hall, 530 Church Street, Ann Arbor, MI 48109-1043, USA

  Email address: `tfylam@umich.edu`